Radiology

REVIEWS AND COMMENTARY • REVIEW

Current and Emerging Knowledge in COVID-19

Yeon Joo Jeong, MD, PhD • Yu Mi Wi, MD, PhD • Hyunjin Park, PhD • Jong Eun Lee, MD • Si-Ho Kim, MD • Kyung Soo Lee, MD, PhD

From the Department of Radiology, Research Institute for Convergence of Biomedical Science and Technology, Pusan National University Yangsan Hospital, Pusan National University School of Medicine, Yangsan, Korea (Y.J.J.); Division of Infectious Diseases, Department of Internal Medicine (Y.M.W., S.H.K.) and Department of Radiology (K.S.L.), Samsung Changwon Hospital, Sungkyunkwan University School of Medicine (SKKU-SOM), Changwon 51353, Korea; Department of Electrical and Computer Engineering, Sungkyunkwan University, Suwon, Korea (H.P.); Center for Neuroscience Imaging Research, Institute for Basic Science, Suwon, Korea (H.P.); and Department of Radiology, Chonnam National University Hospital, Gwangju, Korea (J.E.L.). Received September 26, 2022; revision requested October 17; final revision received November 21; accepted November 23. **Address correspondence to** K.S.L. (email: *kyungs.lee@samsung.com*).

Conflicts of interest are listed at the end of this article.

Radiology 2023; 306(2):e222462 • https://doi.org/10.1148/radiol.222462 • Content code: CH

COVID-19 has emerged as a pandemic leading to a global public health crisis of unprecedented morbidity. A comprehensive insight into the imaging of COVID-19 has enabled early diagnosis, stratification of disease severity, and identification of potential sequelae. The evolution of COVID-19 can be divided into early infectious, pulmonary, and hyperinflammatory phases. Clinical features, imaging features, and management are different among the three phases. In the early stage, peripheral ground-glass opacities are predominant CT findings, and therapy directly targeting SARS-CoV-2 is effective. In the later stage, organizing pneumonia or diffuse alveolar damage pattern are predominant CT findings and anti-inflammatory therapies are more beneficial. The risk of severe disease or hospitalization is lower in breakthrough or Omicron variant infection compared with nonimmunized or Delta variant infections. The protection rates of the fourth dose of mRNA vaccination were 34% and 67% against overall infection and hospitalizations for severe illness, respectively. After acute COVID-19 pneumonia, most residual CT abnormalities gradually decreased in extent, but they may remain as linear or multifocal reticular or cystic lesions. Advanced insights into the pathophysiologic and imaging features of COVID-19 along with vaccine benefits have improved patient care, but emerging knowledge of post–COVID-19 condition, or long COVID, also presents radiology with new challenges.

Supplemental material is available for this article.

SARS-CoV-2, the cause of COVID-19, has spread quickly worldwide and resulted in more than 630 million cases confirmed worldwide and more than 6.6 million deaths as of November 11, 2022 (1). Early detection and management of COVID-19 are challenging because symptoms are nonspecific and the disease spread is quite rapid.

Nucleic acid amplification testing (NAAT) has been the reference standard for detecting COVID-19 due to its near-perfect specificity. However, false-negative results may occur with specimen inadequacy, type, handling, and inappropriate stage of infection when the specimen is acquired (2–4). In this situation, imaging is indicated in patients with COVID-19 with worsening respiratory status or in patients with suspected COVID-19 who present with moderate to severe clinical features (2). With comprehensive insight, imaging, especially chest CT, has played various roles in the pandemic according to the different countries, including diagnosis, triage, and prognosis assessment of patients with COVID-19 pneumonia (5–7).

Vaccination is safe and effective for the prevention of COVID-19 (8). However, inconsistent efficacy for each vaccine platform, waning immunity from the vaccine over time, delayed vaccination in underdeveloped countries, and immune escape by variants (ie, viral mutation that helps the virus evade the human immune system) have resulted in breakthrough infection. Moreover, such a vaccination condition has led to the occurrence of and an increase in highly contagious variants of concern (9–11). Despite effective treatment, some patients can experience long-term effects from their infection, known as post–COVID-19 condition (PCC), or long COVID. Studies are in progress to better understand PCC in terms of risk factors or the role of vaccination to prevent it (12).

This review on the current and emerging knowledge on COVID-19 pneumonia will *(a)* provide a brief overview of the pandemic and the contribution of imaging to the public health crisis, *(b)* inform the advances of knowledge in COVID-19 pneumonia imaging through multiple waves worldwide, and *(c)* summarize the emerging knowledge of PCC.

Pathogenesis with Imaging Correlation

SARS-CoV-2 is an enveloped single positive-strand RNA virus, and its structural proteins serve a crucial role in the pathogenesis of COVID-19 (13). The spike protein has been confirmed as the primary protein that mediates the binding of SARS-CoV-2 to the angiotensin-converting enzyme 2 receptor of the host cells and causes membrane fusion with the assistance of transmembrane protease serine 2. This process serves a key role in viral entry into cells (14,15) (Fig 1). The angiotensin-converting enzyme 2 receptor is highly expressed on the epithelial cells of the oral mucosa and lungs but also in the heart, blood vessels, intestine, kidney, bladder, and brain. Expression of angiotensin-converting enzyme 2 and its affinity are observed to increase with age, which may explain the low severity of COVID-19 in children (16). SARS-CoV-2 is transmitted primarily through close contact with respiratory droplets (17,18). To a lesser extent, it can also be transmitted via aerosols over longer distances (19,20). Unlike severe acute respiratory syndrome coronavirus, which spreads after the onset of symptoms and the contagiousness of which cor-

Abbreviations

ARDS = acute respiratory distress syndrome, CO-RADS = COVID-19 Reporting and Data System, GGO = ground-glass opacity, NAAT = nucleic acid amplification testing, PCC = post–COVID-19 condition

Summary

Advanced insights into the pathophysiology and imaging features of COVID-19 along with vaccine benefits have improved patient care, but emerging knowledge of post–COVID-19 condition (long COVID) also presents radiology with new challenges.

Essentials

- The evolution of COVID-19 can be divided pathophysiologically into three phases: *(a)* early infectious, *(b)* pulmonary, and *(c)* hyperinflammatory; clinical and imaging features and management are different according to each phase.
- The adjusted protection rates of the fourth dose of mRNA vaccination were 34%, 67%, and 72% against overall infection, hospitalizations for severe illness, and related deaths during the Omicron surge.
- The most common CT findings of COVID-19 pneumonia are ground-glass opacity with or without interlobular septal thickening, consolidation, or a combination of both, usually located in the peripheral lung and often in peribronchial areas, which progressively evolve toward organizing pneumonia pattern; the imaging findings of breakthrough infections seem to be similar to those in unvaccinated patients, albeit generally less severe, and immunized patients seem to be at lower risk of requiring supplemental oxygen or intensive care unit admission.
- Clinical symptoms and disease severity of COVID-19 can vary depending on the type of variant, and the Omicron variant had a lower risk of CT pneumonia severity and clinical severity than the Delta variant.
- Although only a small portion of patients with post–COVID-19 condition (ie, long COVID) have radiologic abnormalities, CT features seen at 1-year follow-up studies are fibrotic-like linear or multifocal reticular or cystic lesions admixed with ground-glass opacity, and the extent of lesions is correlated with lung diffusion abnormality.

responds to the disease severity, viral shedding of SARS-CoV-2 begins before the onset of symptoms and peaks in the 1st week of symptoms before the infected host becomes seriously ill (21). These unique virologic characteristics have made SARS-CoV-2 an unprecedented virus, causing a pandemic.

It is hypothesized that SARS-CoV-2 infection goes through the following three stages: *(a)* early infection (viral invasion and replication), *(b)* pulmonary phase (host inflammatory response), and *(c)* hyperinflammatory phase (dysregulated immune response) (22) (Fig 1). Clinical features, imaging features, and management are different according to each phase. After the virus enters the cells, the viral RNA genome is released and replicated. Its antigen is then presented to dendritic cells or macrophages that stimulate the body's humoral and cellular immunity by virus-specific B and T cells (23). Virus-specific B and T cells produce antibodies and release numerous cytokines, which induce and amplify the inflammatory response (Fig 1). An uncontrolled systemic inflammatory response resulting from the release of a large amount of proinflammatory cytokines, called a cytokine storm, causes acute respiratory distress syndrome (ARDS) and multiorgan failure in a minority of infections (Fig 2).

A rapid decline of natural- and vaccine-induced immunity and low neutralizing activity with existing vaccines against new variants has been observed (24–27). A predictive model of immune protection from COVID-19 estimated that the waning of neutralization titer over time has nonlinear effects on the level of protection, depending on initial vaccine efficacy (28,29). Although a substantial waning of neutralization after 250 days will occur, it slows linearly over 2 years, which seems to reduce the risk of hospitalization or severe disease (30,31). In general, it is assumed that the viral evolution proceeds in the direction of decreasing mortality to increase transmissibility. However, the Delta variant has higher mortality than previous emerging variants but effectively transmits during the early periods of disease progression (32). The Omicron (B.1.1.529) variant and its sublineages have become the globally dominant variants as of October 2022 (33,34). The Omicron variant and its sublineages are more transmissible than the Delta variant and are associated with a higher risk of repeat infection (Fig 3A, 3B) in individuals previously infected with wild-type or other variants that have been previously circulating variants of concern (eg, Alpha, Beta, Gamma, and Delta) and breakthrough infection (26,27,35–37) (Fig 3C). These may be related to higher angiotensin-converting enzyme 2 binding affinity and immune escape phenomenon due to more mutations in the spike protein of the Omicron variant. However, the adjusted protection rates of the fourth dose of mRNA vaccination were 34%, 67%, and 72% against overall infection, hospitalizations for severe illness, and related deaths during the Omicron surge (38). A close monitoring for new variant emergence of SARS-CoV-2 should be emphasized, despite the prevailing optimism based on assumptions of the viral evolution and immunity acquired through natural infection and vaccination.

Imaging of COVID-19 Pneumonia

At Diagnosis and during Disease Stages

According to the World Health Organization (WHO), one of the following two conditions must be satisfied for the definition of confirmed SARS-CoV-2 infection: *(a)* the patient receives a positive finding at NAAT regardless of clinical or epidemiologic criteria or *(b)* the patient meets clinical and/or epidemiologic criteria with a positive SARS-CoV-2 antigen test (39). NAAT is a viral diagnostic test that helps detect viral RNA with high sensitivity and specificity; however, a long turnaround time (up to 2 days) is needed. Chest imaging has an auxiliary role in diagnosing COVID-19. However, the WHO suggests that chest imaging may be considered in specific cases, as follows: *(a)* when NAAT is not available, *(b)* when the NAAT result is delayed, and (*c)* in a patient with a negative result at NAAT in whom COVID-19 is highly suspicious (40).

Imaging is not routinely indicated as a screening test for COVID-19 in asymptomatic individuals or for patients with mild features unless they are at risk for disease progression (2). Although less sensitive than chest CT, chest radiography is typically the first-line imaging modality used for patients with COVID-19 (2).

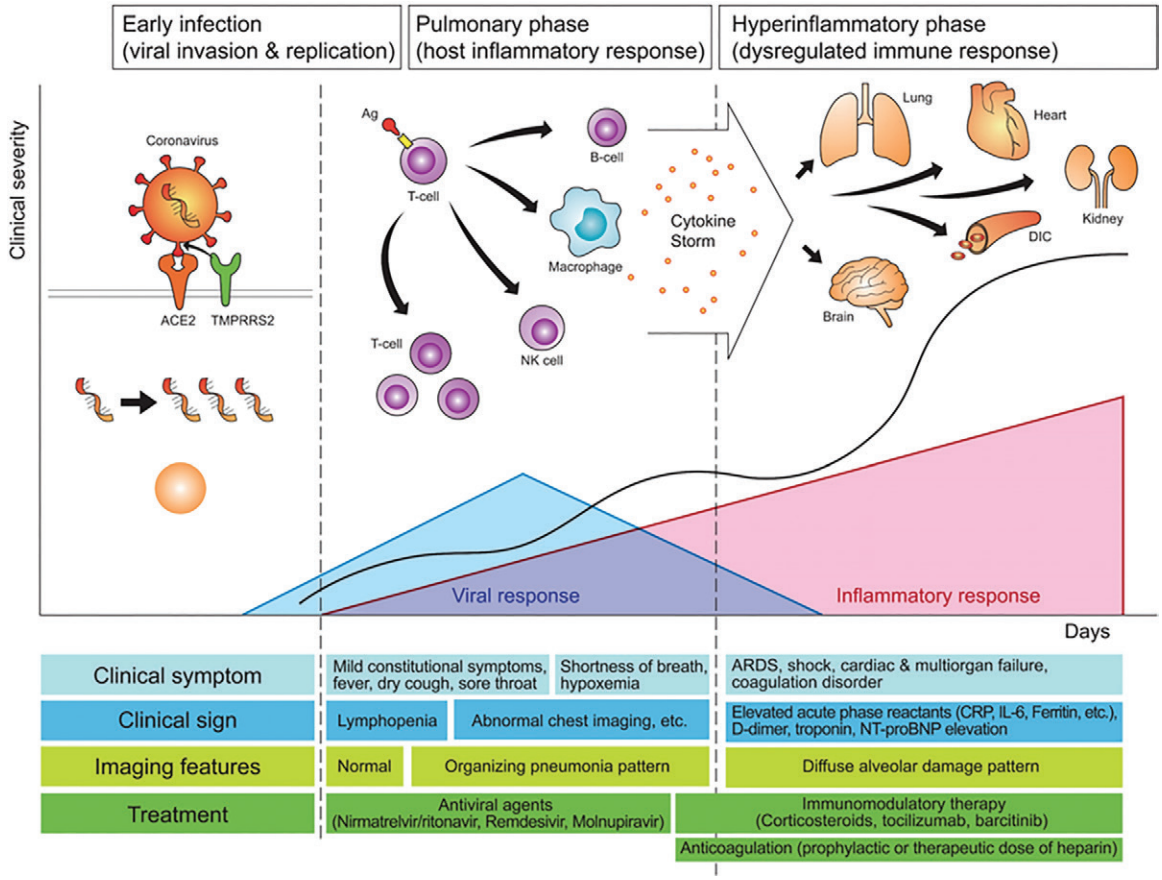

Figure 1: Diagram shows how pathogenetic evolution of COVID-19 pneumonia correlates with clinical and imaging features and management. The early infection stage occurs at the time of inoculation. During this stage, SARS-CoV-2 binds to its target using the angiotensin-converting enzyme 2 (ACE2) receptor and transmembrane protease serine 2 (TMPRRS2) and multiplies in the host cells. In the second stage, the pulmonary phase, viral multiplication and localized inflammation in the lungs occur and viral pneumonia is developed. In a minority of patients with COVID-19, the disease may progress to the most severe stage, the hyperinflammatory phase. An uncontrolled systemic inflammatory response resulting from the cytokine storm occurs at this stage. Pink triangle indicates inflammatory response, blue triangle indicates viral response, and black line indicates clinical severity. Areas under trigon represent chronological changes in the intensity of responses. Ag = antigen, ARDS = acute respiratory distress syndrome, CRP = C-reactive protein, DIC = disseminated intravascular coagulation, IL-6 = interleukin-6, NT-proBNP = *N*-terminal prohormone of brain natriuretic peptide.

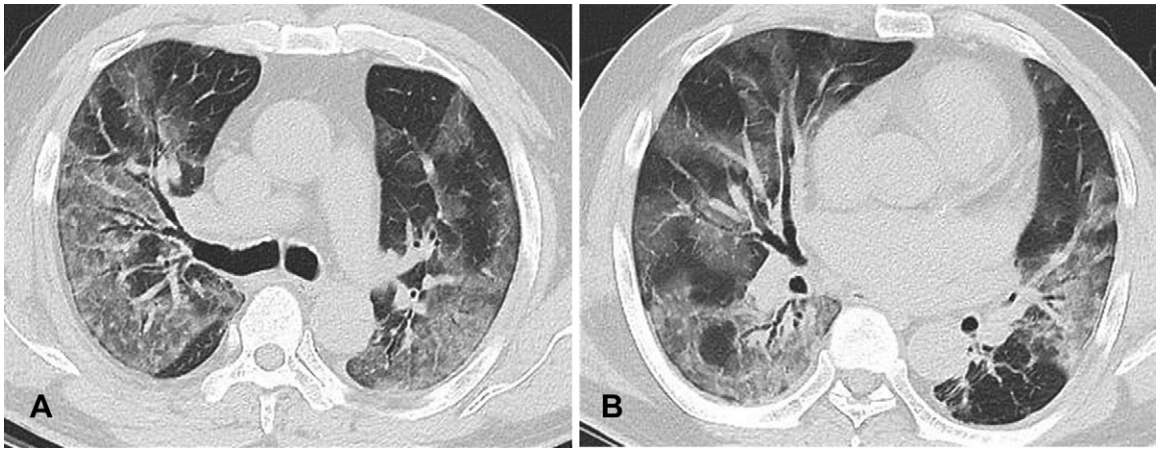

Figure 2: COVID-19 pneumonia with diffuse alveolar damage pattern in a 64-year-old unvaccinated man with no underlying disease at Delta variant–dominant period. **(A, B)** Follow-up transverse nonenhanced CT scans (lung window) obtained at levels of right main bronchus **(A)** and right middle lobar bronchus **(B)** 1 day after positive nucleic acid amplification test for COVID-19 demonstrate extensive areas of ground-glass opacity involving bilateral lungs.

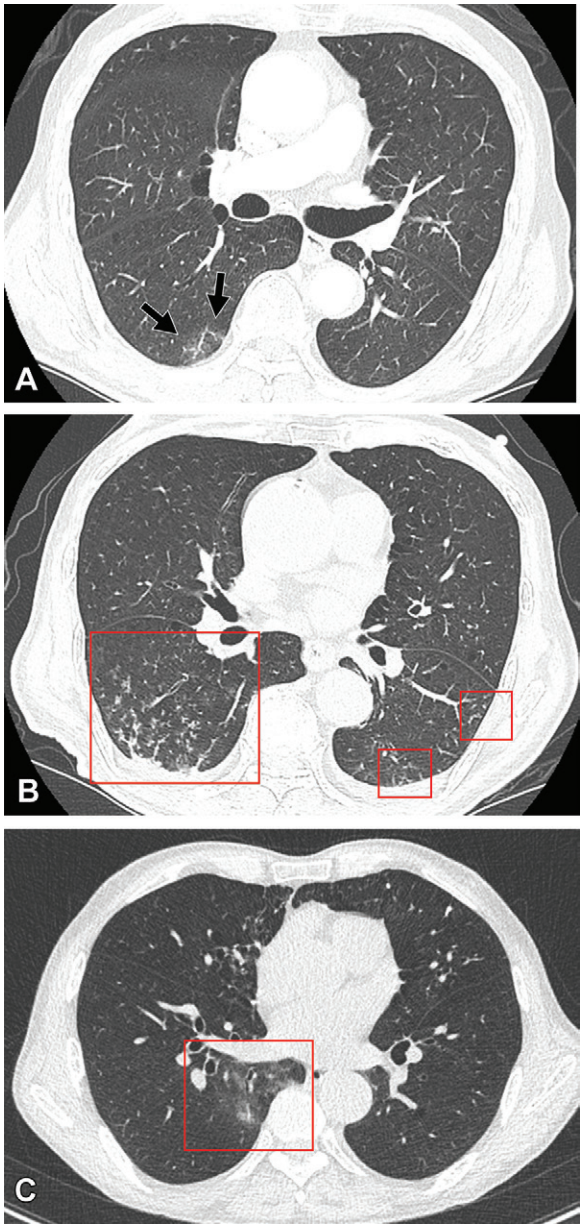

Figure 3: Cases of SARS-CoV-2 reinfection and breakthrough infection during an Omicron BA.5 subvariant–predominant period. **(A, B)** CT scans (lung window) in an 82-year-old man with COVID-19 reinfection during an Omicron BA.5 subvariant predominant period. The patient had a history of prior Omicron BA.1 subvariant infection and cerebrovascular accident. **(A)** Transverse nonenhanced CT scan obtained at bronchus intermedius level at the time of Omicron BA.1 subvariant (his first infection) shows focal area of ground-glass opacity (GGO) in superior segment of right lower lobe (arrows). CT findings were classified as "indeterminate" according to the RSNA chest CT classification system. **(B)** Transverse nonenhanced CT scan obtained at the level of basal trunks at the time of reinfection of Omicron BA.5 subvariant 4 months after the first infection shows poorly defined centrilobular nodules in the dependent portions of bilateral lower lobes (squares). CT findings were classified as "atypical" according to the RSNA chest CT classification system. **(C)** CT scan (lung window) of breakthrough infection of SARS-CoV-2 during an Omicron BA.1 subvariant–dominant period in a 76-year-old man with a history of hypertension and pulmonary tuberculosis who had received his COVID-19 booster. Transverse nonenhanced CT scan obtained at level of inferior pulmonary vein shows focal area of poorly defined GGO (square) in the right lower lobe. CT findings were classified as "indeterminate" according to the RSNA chest CT classification system.

Clinical and imaging manifestations usually depend on the disease stage (22) (Fig 1). The disease progression rate among patients with COVID-19 differs by age, underlying medical conditions, immune status, variant type, and vaccination status (22). Systemic manifestations can be present because of an autoimmunity against angiotensin-converting enzyme 2 widely distributed (29,41) in human cells and the initiation of proinflammatory cytokines release (42). During early infection, chest radiographs may be normal (Fig 4A, 4B). In unvaccinated patients with COVID-19 requiring hospitalization, 37% (279 of 761) had an abnormal chest radiograph at the initial time of admission and 46% (298 of 653) had radiographic abnormalities during hospitalization (43).

In the pulmonary phase, viral pneumonia appears. The most frequent chest radiographic findings of COVID-19 pneumonia are multifocal consolidation or ground-glass opacity (GGO), usually with bilateral, peripheral, and lower zone predominance (44) (Fig 4C, 4D). Pleural effusion is rare (6%) (44).

In the hyperinflammatory phase, a minority of patients with COVID-19 can show progressive disease to ARDS and multiorgan failure. A prospective cohort study reported that 24% of hospitalized patients with COVID-19 required mechanical ventilation in the prevaccine era (45). In the hyperinflammatory phase, parenchymal abnormalities undergo spread to both sides of the lungs with a greater extent of involvement (Fig 4E, 4F). Greater extent of parenchymal lesions or higher radiographic scores are strongly associated with admission to the intensive care unit or death (Figs 2, 4E, 4F). In particular, when the extent of the parenchymal lesion is greater than 75%, the risk of intensive care unit admission or death is three to four times higher than when extent is less than 25% (46). Systemic steroid therapy targeting COVID-19–induced hyperinflammatory response improves prognosis and reduces mortality in hospitalized patients requiring supplemental oxygen (47,48) (Table S1).

CT Findings and Classification Systems and Structured Report Proposals for COVID-19 Pneumonia

CT can be used in the diagnosis of COVID-19 and is an important complement to NAAT (7). During the early period of the outbreak, the reported sensitivity of chest CT was 97% based on positive NAAT (49) and 98% of patients had evidence of abnormal CT compatible with viral pneumonia at baseline, while the sensitivity of NAAT was 71% (50). In another study (51), when using predefined criteria (positive or negative for COVID-19), CT interpretation performance was not influenced by reader experience and enabled a correct diagnosis of COVID-19 pneumonia with an overall accuracy of 80%.

The most common CT findings of COVID-19 pneumonia are GGO with or without interlobular septal thickening, consolidation, or a combination of both (Figs 4D, 4F, 5A–5D), usually located in the peripheral lung (Figs 4D, 5A–5C) and often in peribronchial areas, which progressively evolve toward organizing pneumonia pattern (subpleural and/or peribronchial distributed consolidation and GGO) (52,53) (Fig 5A, 5B).

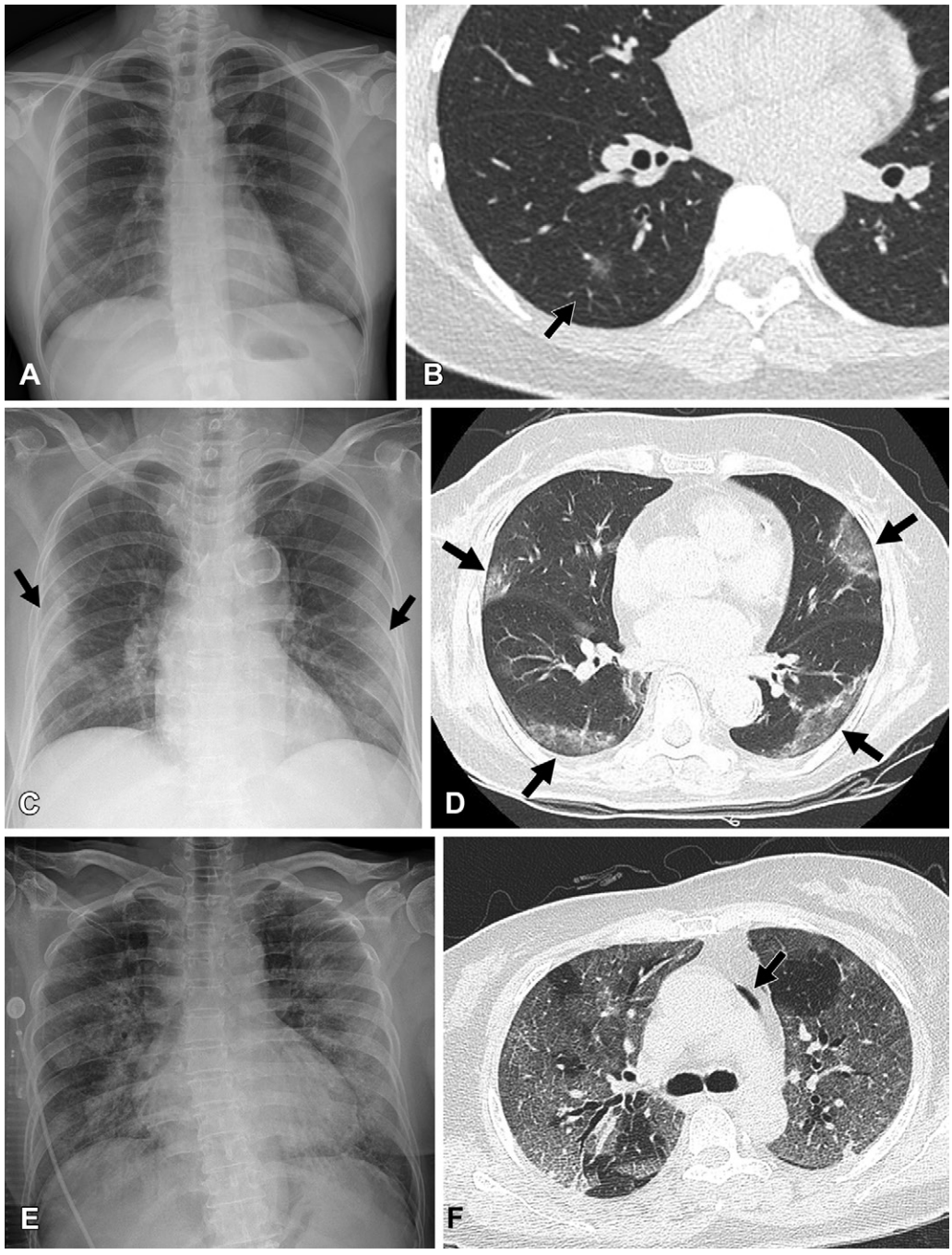

Figure 4: Chest radiographic and CT findings of COVID-19 pneumonia according to disease stage and lesion extent. **(A, B)** COVID-19 pneumonia at the time of "early infection phase" in a 42-year-old woman who received a booster dose during Omicron variant–dominant period. **(A)** Chest radiograph obtained 3 days after the positive nucleic acid amplification test shows no abnormal opacification in either lung. **(B)** Transverse nonenhanced CT scan (lung window) obtained at level of basal trunk and on the same day shows an ill-defined ground-glass opacity (GGO) nodule (arrow) in the superior segment of the right lower lobe. **(C, D)** COVID-19 pneumonia at the time of "pulmonary phase" in an 80-year-old fully vaccinated woman during Delta variant–dominant period. **(C)** Chest radiograph obtained 5 days after positive nucleic acid amplification test shows multifocal patchy consolidation and GGO (arrows) in both lungs with a peripheral predominance. **(D)** Transverse nonenhanced CT scan (lung window) obtained at the level of the inferior pulmonary vein and on the same day demonstrates patchy areas of mixed GGO and consolidation with subpleural distribution (arrows). **(E, F)** COVID-19 pneumonia at the time of "hyperinflammatory phase" in a 69-year-old unvaccinated woman with no underlying disease during Delta variant–dominant period. **(E)** Chest radiograph obtained 2 weeks after positive nucleic acid amplification test shows diffuse and extensive parenchymal opacity involving bilateral lungs. **(F)** Transverse nonenhanced CT scan (lung window) obtained at the level of carina and on the same day demonstrates diffuse and extensive areas of GGO with visible intralobular lines involving bilateral lungs. Also note pneumomediastinum at left paraaortic area (arrow). Even though the patient was treated with mechanical ventilation and extracorporeal membrane oxygenation, she succumbed to the disease.

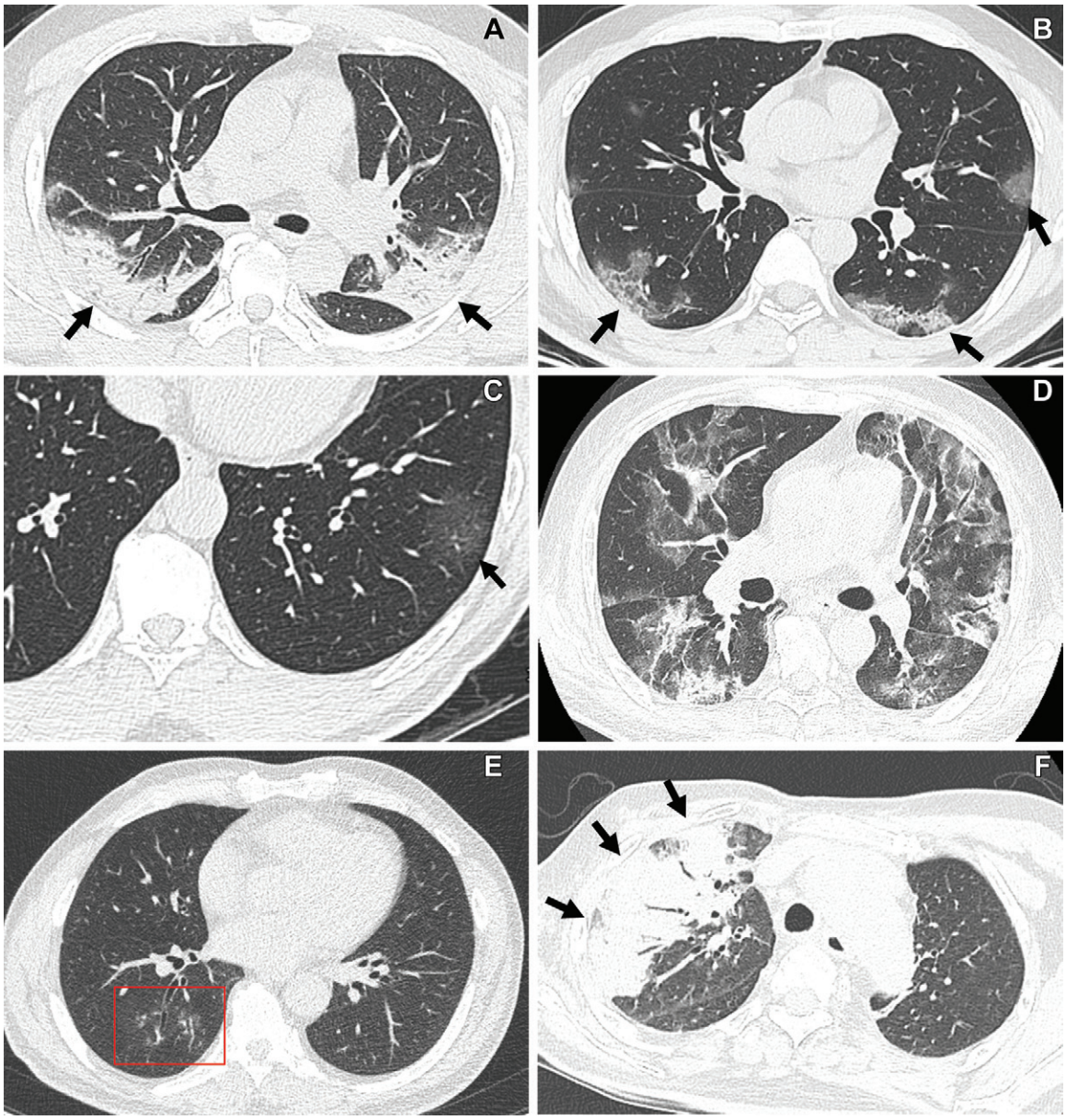

Figure 5: CT findings of COVID-19 pneumonia according to RSNA CT classification schemes. **(A, B)** "Typical" COVID-19 pneumonia according to the RSNA chest CT classification system. **(A)** Transverse nonenhanced CT scan (lung window) obtained in a 48-year-old unvaccinated man with a history of hypertension and diabetes seen at the wild type–dominant period shows bilateral areas of consolidation with peripheral distribution (arrows). **(B)** Transverse nonenhanced CT scan (lung window) obtained in a 40-year-old unvaccinated man with no underlying disease seen at the wild type–dominant period shows patchy areas of mixed ground-glass opacity (GGO) and consolidation with subpleural distribution (arrows). **(C, D)** "Indeterminate" COVID-19 pneumonia according to the RSNA chest CT classification system. **(C)** Transverse nonenhanced CT scan (lung window) obtained in a 61-year-old unvaccinated woman with no underlying disease seen at the wild type–dominant period shows focal area of GGO (arrow) in left lower lobe. **(D)** Transverse nonenhanced CT scan (lung window) obtained in a 65-year-old fully vaccinated man with hypertension, diabetes, and a history of renal transplant seen at the Delta variant–dominant period shows extensive areas of mixed GGO and consolidation without zonal predominance. **(E, F)** "Atypical" COVID-19 pneumonia according to the RSNA chest CT classification system. **(E)** Transverse nonenhanced CT scan (lung window) obtained in a 42-year-old woman who received a booster dose with no underlying disease seen at Omicron variant–dominant period shows poorly defined small nodules (box) with peribronchial distribution in the right lower lobe. **(F)** Transverse nonenhanced CT scan (lung window) obtained in a 68-year-old unvaccinated man with history of cerebrovascular accident seen at Omicron variant–dominant period shows segmental area of consolidation (arrows) with air bronchogram in the right upper lobe.

Cavity, centrilobular small nodules (Fig 5E), segmental or lobar consolidation (Fig 5F), and mediastinal or hilar lymph node enlargement are rarely seen in COVID-19. Pulmonary vascular enlargements in areas of lung opacity can be seen (54). As the disease progresses, parenchymal abnormalities eventually spread to involve both lungs and appear as a diffuse alveolar damage pattern (bilateral diffuse GGO and consolidation) (Figs 2, 4F).

To facilitate accurate imaging diagnosis and reduce radiologists' variability in the reporting of chest CT findings, various structured reports for COVID-19 have been proposed (54–57) (Table 1).

Table 1: Comparison between Different Chest CT Classification Systems in COVID-19

COVID-19 Level of Suspicion	RSNA	CO-RADS	COVID-RADS	BSTI
Not interpretable	Not categorized	CO-RADS 0	Not categorized	Not categorized
Very low	Negative for pneumonia	CO-RADS 1: normal	COVID-RADS 0: normal	Normal (correlates with RT-PCR)
Low	Atypical appearance (uncommon and/or not reported features for COVID-19)	CO-RADS 2: typical for other infections	COVID-RADS 1: atypical findings (inconsistent with COVID-19)	Non–COVID-19 (level of confidence for alternative: 70%)
Unsure or equivocal	Indeterminate appearance (nonspecific features of COVID-19)	CO-RADS 3: features compatible with COVID but present in other diseases	COVID-RADS 2A: fairly typical findings	Indeterminate (level of confidence for COVID-19: <70%)
High	Indeterminate appearance (nonspecific features of COVID-19)	CO-RADS 4: suspicious	COVID-RADS 2B: combination of atypical findings with typical and/or fairly typical findings	Probable COVID-19 (level of confidence for COVID-19: 71%–99%)
Very high	Typical appearance (commonly reported imaging findings; highly specific for COVID-19)	CO-RADS 5: typical	COVID-RADS 3: typical findings	Classic COVID-19 (level of confidence for COVID-19: 100%)
Proven	Not categorized	CO-RADS 6: confirmed diagnosis: RT-PCR for SARS-CoV-2	Not categorized	Not categorized

Note.—BSTI =British Society of Thoracic Imaging statement guideline, CO-RADS = COVID-19 Reporting and Data System, COVID-RADS = COVID-19 Imaging Reporting and Data System, RSNA = RSNA expert consensus statement category, RT-PCR = reverse-transcription polymerase chain reaction. Table modified, under a CC BY license, from reference 118.

RSNA chest CT classification system for reporting COVID-19 pneumonia.—The RSNA published an expert consensus statement on chest CT reporting of COVID-19 (56). The statement proposes four categories for the suggested standardized CT reporting language of COVID-19, as follows: typical (Fig 5A, 5B), indeterminate (Fig 5C, 5D), atypical appearance (Fig 5E, 5F), and negative for pneumonia (Table S2). This classification provided radiologists and referring providers guidance and confidence in reporting these findings and a more consistent framework to improve clarity.

COVID-19 Reporting and Data System.—The COVID-19 Reporting and Data System (CO-RADS) also provides a standardized assessment scheme with a five-point scale of suspicion for reporting nonenhanced chest CT scans from patients under investigation for COVID-19 (55). The main strengths of CO-RADS are its interobserver agreement (moderate to substantial agreement) and its ability to distinguish between the low and high probability of COVID-19. The use of CO-RADS and CT severity scores is useful for the triage, diagnosis, and management decisions of patients presenting with possible COVID-19 at the emergency department (58).

European classification systems for the structured report of COVID-19 pneumonia.—The COVID-19 Imaging Reporting and Data System (COVID-RADS) is a relatively simplified reporting system based on a combination of findings with different levels of suspicion (54). This system classified the CT findings of COVID-19 pneumonia into five categories: typical findings, the combination of atypical findings with typical and/or fairly typical findings, fairly typical findings, atypical findings, and normal. It also suggested a common lexicon. The British Society of Thoracic Imaging proposed a similar initiative while also adding a descriptor for disease severity, making the distinction between mild and moderate and/or severe disease, although this effort is not based on evidence regarding patient outcome (57).

Which of the above-mentioned structured reporting systems to use or how to integrate them for patients care depends on the reproducibility, reliability, and simplicity of these reporting systems. The more widely used of these reporting systems, RSNA classification system and CO-RADS, are comparable in diagnosis of COVID-19 pneumonia with similar sensitivity (overall sensitivity, 72.7%; sensitivity for patients with severe disease, approximately 94.7%–97.8%) and reliability (59). However, the CO-RADS has a better interobserver agreement (κ = 0.801 vs 0.781) that may be attributed to greater familiarity with the CO-RADS among radiologists due to its resemblance to other reporting and data systems.

Special Considerations

Breakthrough Infections

The reported incidences of COVID-19 breakthrough infection, the development of active COVID-19 in previously vaccinated individuals, range from 0.4% to 9.5%, depending on

Table 2: Differences in Phenotypic Characteristics and Clinical and Imaging Findings between SARS-Cov-2 Delta and Omicron Variants

Characteristic	Delta Variant (B.1.617.2)	Omicron Variant (B.1.1.529)
Phenotypic characteristics		
Transmissibility	Increased transmissibility compared with wild-type virus (34)	Sublineages BA.1 and BA.2: increased transmissibility compared with Delta (34) Sublineages BA.4 and BA.5: uncertain impact on transmissibility compared with other Omicron sublineages (35)
Immune escape	Reduced neutralization by convalescent and postvaccination sera compared with wild-type virus (24)	Sublineages BA.1 and BA.2: more reduction in neutralization by convalescent and postvaccination sera than Delta (27,38) Sublineages BA.4 and BA.5: more reduction in neutralization by convalescent and postvaccination sera than BA.1 and BA.2 (37,116)
Clinical and imaging findings		
Prevalence of symptoms (64)	Reference	Less common classic COVID-19 symptoms* (OR, 0.56; 95% CI: 0.51, 0.61), more common sore throat (OR, 1.55; 95% CI: 1.43, 1.69)
Risk of hospitalization (64)	Reference	Reduced risk of hospitalization (OR, 0.75; 95% CI: 0.57, 0.98)
Risk of PCC (99)	Reference	Reduced risk of PCC (OR, 0.24–0.50 depending on age and time since vaccination)
Severity of CT pneumonia (67)	Reference	Lower severity of pneumonia (OR, 0.71; 95% CI: 0.51, 0.99)
Rates of CT pneumonia patterns (67,68,117)	Reference	Lower rates of RSNA typical chest CT findings (32%–40% vs 57%–83%), higher rates of RSNA atypical chest CT findings (13%–28% vs 1.5%–3%)

Note.—OR = odds ratio, PCC = post–COVID-19 condition (long COVID), RSNA = RSNA expert consensus statement category.
* Fever, loss of smell, and persistent cough.

the vaccine type, the time elapsed after vaccination, the percentage of vaccinated people, and viral variants (43,60–63). The imaging findings of breakthrough infections seem to be similar to those in unvaccinated patients, albeit generally less severe (Fig 3C). In hospitalized patients with COVID-19, a higher percentage of fully vaccinated patients had no pneumonia on CT scans (unvaccinated patients vs fully vaccinated patients, 22% vs 59%) (43). In addition, immunized patients seem to be at lower risk of requiring supplemental oxygen or intensive care unit admission.

Differences in Imaging Findings between Variants of SARS-CoV-2

Clinical symptoms and disease severity of COVID-19 can vary depending on the type of variant (Table 2). Loss of smell is more common with the Delta variant, while a sore throat is more common with the Omicron variant (64). Although the Omicron variant has a high replication and immune evasion ability (65), the rates of hospitalization, mortality, and persistent COVID-19 symptoms were lower than those of the Delta variant in observational studies (64,66).

In 2180 hospitalized patients with COVID-19, CT was more likely to be negative for pneumonia during periods of Omicron versus Delta variant prevalence (71% vs 35%, respectively; $P < .001$), and the Omicron variant had a lower risk of CT pneumonia severity (odds ratio, 0.71; $P = .04$) and clinical severity (odds ratio, 0.43; $P = .004$) than the Delta variant (67) (Fig 6). The proportion of patients with an atypical CT pattern was higher in the Omicron variant group than in the Delta variant group (67,68) (Table 2) (Fig 6D).

Repeat Infection

After recovering from COVID-19, most individuals will have some protection from repeat infections. However, repeat infections do occur after COVID-19. In retrospective cohort studies, the incidence of repeat infection is approximately 0.2%–0.3% and has increased from the pre-Delta period to the Omicron period (6.0 per 100 000 persons vs 355 per 100 000 persons) (69,70). Repeat infections are more likely in women, adults, immunocompromised patients, and those previously hospitalized for COVID-19 (71). Full vaccination provides additional protection against repeat infection (72). It has been reported that breakthrough infections with the Omicron BA.5 subvariant were less likely among persons with prior SARS-CoV-2 infection, especially for previous BA.1 or BA.2 infection, with a protective efficacy of 75%, compared with uninfected persons (73).

Although imaging findings of repeat infections with SARS-CoV-2 have not been fully reported, reinfection or relapse of COVID-19 may have imaging findings similar to the pneumonia when the variants were prevalent at the time (Fig 3A, 3B). According to a 2021 report (74), CT showed a resolution of pulmonary involvement between the two episodes with new and progressive changes during reinfection. Therefore, it is important to obtain new baseline images in patients with COVID-19 at the

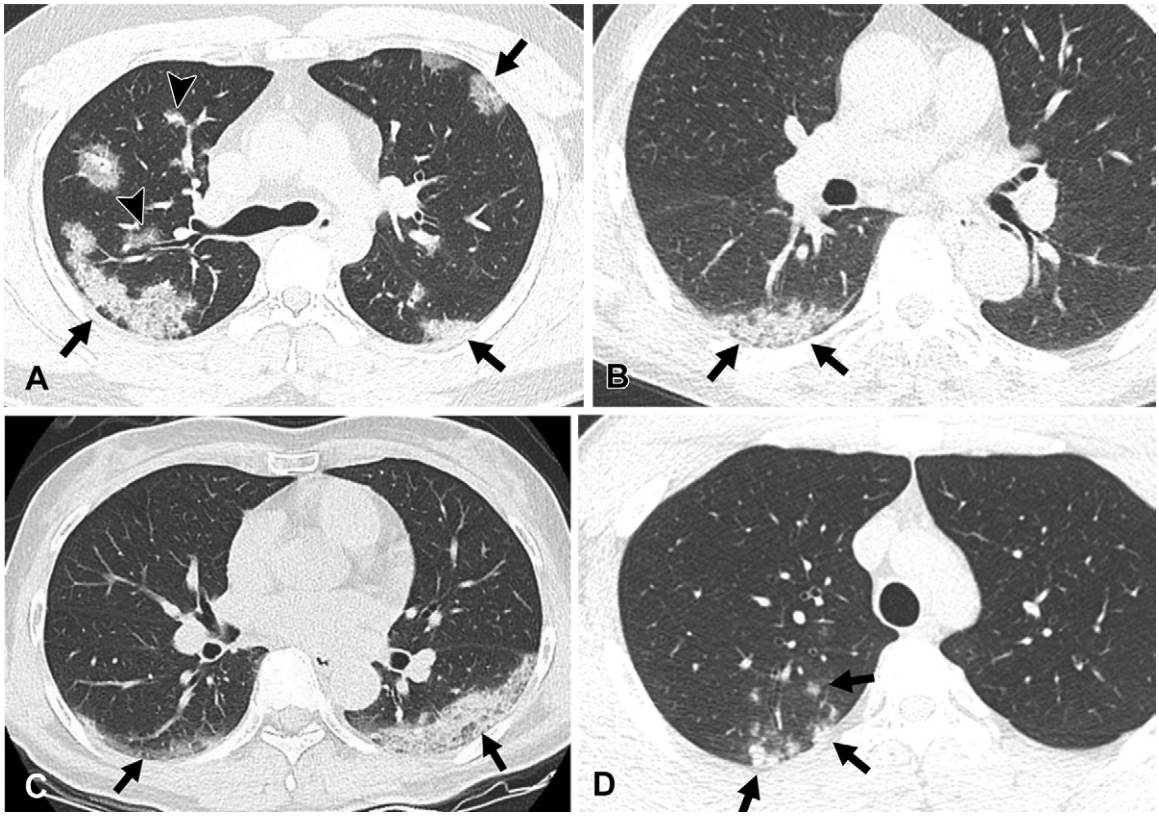

Figure 6: COVID-19 pneumonia during Delta variant– and Omicron variant–dominant periods. **(A, B)** Images of COVID-19 pneumonia at Delta variant–dominant period. **(A)** Transverse nonenhanced CT scan (lung window) obtained in a 34-year-old unvaccinated man with no underlying disease shows multifocal areas of mixed ground-glass opacity (GGO) and consolidation with subpleural (arrows) and peribronchial (arrowheads) distribution. CT findings were classified as "typical" according to the RSNA chest CT classification system. **(B)** Transverse nonenhanced CT scan (lung window) obtained in a 58-year-old fully vaccinated man with no underlying disease seen at Delta variant–dominant period shows a focal subpleural area of consolidation (arrows) in superior segment of right lower lobe. This case was classified as "indeterminate" according to the RSNA chest CT classification system. **(C, D)** COVID-19 pneumonia at Omicron variant–dominant period. **(C)** Transverse nonenhanced CT scan (lung window) obtained in 56-year-old unvaccinated woman with no underlying disease shows subpleural areas of mixed GGO and consolidation (arrows) in both lower lobes. CT findings were classified as "typical" according to the RSNA chest CT classification system. **(D)** Transverse nonenhanced CT scan (lung window) obtained in a 20-year-old man with no underlying disease who received a booster dose shows poorly defined centrilobular nodules in the right upper lobe (arrows). This case was considered "atypical" according to the RSNA chest CT classification system.

time of hospital discharge or clinical recovery. This new reference can help determine whether readmissions are from relapse or reinfection of COVID-19 or a different viral infection and also aid in understanding the long-term sequelae of COVID-19 (75).

Immunocompromised Patients

The clinical features and outcomes of COVID-19 among immunocompromised patients related to risk factors for severe disease or reduced detrimental inflammatory responses are not well characterized. Patients with hematologic malignancy do show prolonged viral shedding and higher mortality compared with the general population or patients with solid tumors (76). A national cohort study from the United Kingdom suggests that people living with HIV have 2.9-fold higher mortality than those without HIV (77). The available data suggest that solid organ recipients or patients with rheumatic disease also have higher mortality, but these results may be primarily driven by a higher comorbidity burden (78,79). In 51 consecutive lung transplant recipients hospitalized with COVID-19, lung transplant recipients had a significantly higher proportion of indeterminate CT pattern (0.31 vs 0.11; $P = .014$) and more severe parenchymal disease (0.372 vs 0.148, $P < .001$) than nontransplanted controls (80) (Fig 7).

Twindemic: COVID-19 and Influenza

Although nonpharmaceutical interventions (eg, social distancing and respiratory etiquette) suppressed the burden of influenza during the COVID-19 pandemic (81), concerns of a "twindemic" (COVID-19 and influenza) have increased. From April to July 2022, Australia experienced a bad flu season, exceeding the 5-year average of laboratory-confirmed influenza (82). Coinfection could affect disease severity. Observational data suggest that patients co-infected with SARS-CoV-2 and influenza have higher odds ratios (4.14 and 2.35, respectively) for invasive mechanical ventilation and in-hospital mortality than those infected with SARS-CoV-2 only. The identification of influenza infection in the background of COVID-19 pneumonia is difficult, as both can manifest with bilateral peripheral GGO and consolidation at CT. However, bronchiectasis and pleural effusion are more often associated with influenza, whereas crazy-paving appearance, lin-

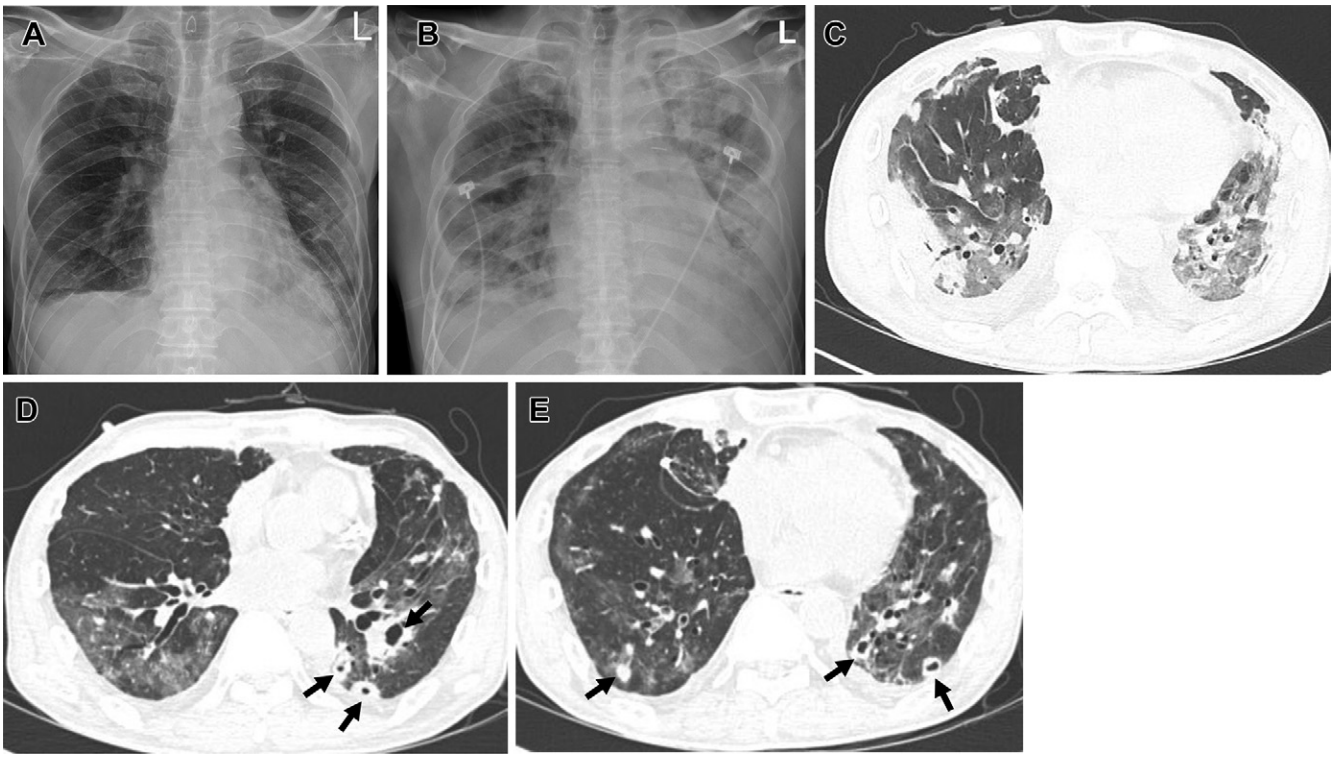

Figure 7: COVID-19 pneumonia during an Omicron BA.5 subvariant–predominant period in a 58-year-old man with a history of lung transplant for idiopathic pulmonary fibrosis who had received a booster dose of vaccine. **(A)** Chest radiograph obtained 7 days after positive nucleic acid amplification test for COVID-19 shows parenchymal opacity involving peripheral portion of both lower lungs. **(B)** Follow-up chest radiograph obtained 2 days after the initial chest radiograph demonstrates increased parenchymal opacity and extensive consolidation in the lungs. **(C)** Transverse nonenhanced CT scan (lung window) obtained at the level of segmental bronchi of both lower lobes 9 days after SARS-CoV-2 infection demonstrates extensive areas of mixed ground-glass opacity (GGO) and consolidation, with a peripheral predominance. **(D, E)** Follow-up transverse nonenhanced CT scans (lung window) obtained at levels of inferior pulmonary veins **(D)** and segmental bronchi of both lower lobes **(E)** 3 weeks after SARS-CoV-2 infection demonstrate decreased extent of GGO and consolidation, but multiple nodules (arrows) with or without cavity are scattered in bilateral lungs. Galactomannan antigen test for *Aspergillus* was positive at this time. The patient died with acute respiratory distress syndrome.

ear opacification, and vascular enlargement are more common in COVID-19 pneumonia (83).

Complications and Their Clinical and Imaging Features

Intensive Care and Ventilation Therapy

Patients showing a diffuse alveolar damage pattern at CT have clinically severe disease, thus requiring oxygen or mechanical ventilation therapy (5) (Fig 8). The consequent patterns of oxygen toxicity and ventilation therapy include areas of reticular and GGO in addition to pulmonary cysts of varying sizes and bullae, particularly in the anterior parts of the lungs in some patients (84). These findings are similar to the fibrosing stage of diffuse alveolar damage (Fig 8C).

Patients with COVID-19 with diffuse alveolar damage are thought to be more vulnerable to barotrauma compared with patients with ARDS due to other than COVID-19 causes (85). Pneumothorax and pneumomediastinum are representative complications caused mainly by barotrauma, especially in patients with other lung abnormalities (Fig 8). A higher-than-expected incidence of pneumothorax or pneumomediastinum has also been observed in patients with COVID-19 not requiring invasive mechanical ventilation (86). These findings may be related to the existence of virus-induced frailty of lung parenchyma, possibly triggered by microvascular thrombosis, interstitial inflammation, and endothelial barrier disruption. Paternoster and colleagues (87) evaluated the role of the Macklin effect, which is a perceptible crescent collection of air contiguous to the bronchovascular sheath, on chest CT images in predicting the subsequent occurrence of pneumomediastinum and/or pneumothorax in patients with COVID-19 (Fig 8C). The Macklin effect was observed in 5% of patients who had diffuse alveolar damage patterns at CT. The Macklin effect yielded a sensitivity of 100%, a specificity of 99.9%, a positive predictive value of 96.7%, a negative predictive value of 100%, and an accuracy of 99.8% in predicting pneumomediastinum and/or pneumothorax. Moreover, all patients with observed Macklin effect developed ARDS necessitating intensive care unit admission, and 90% of these patients required invasive mechanical ventilation.

Superinfection

In patients with a diffuse alveolar damage pattern at CT, a condition of prolonged stay in the intensive care unit, early and inappropriate use of corticosteroids, virus-induced immune dysregulation, and concurrent use of immunomodula-

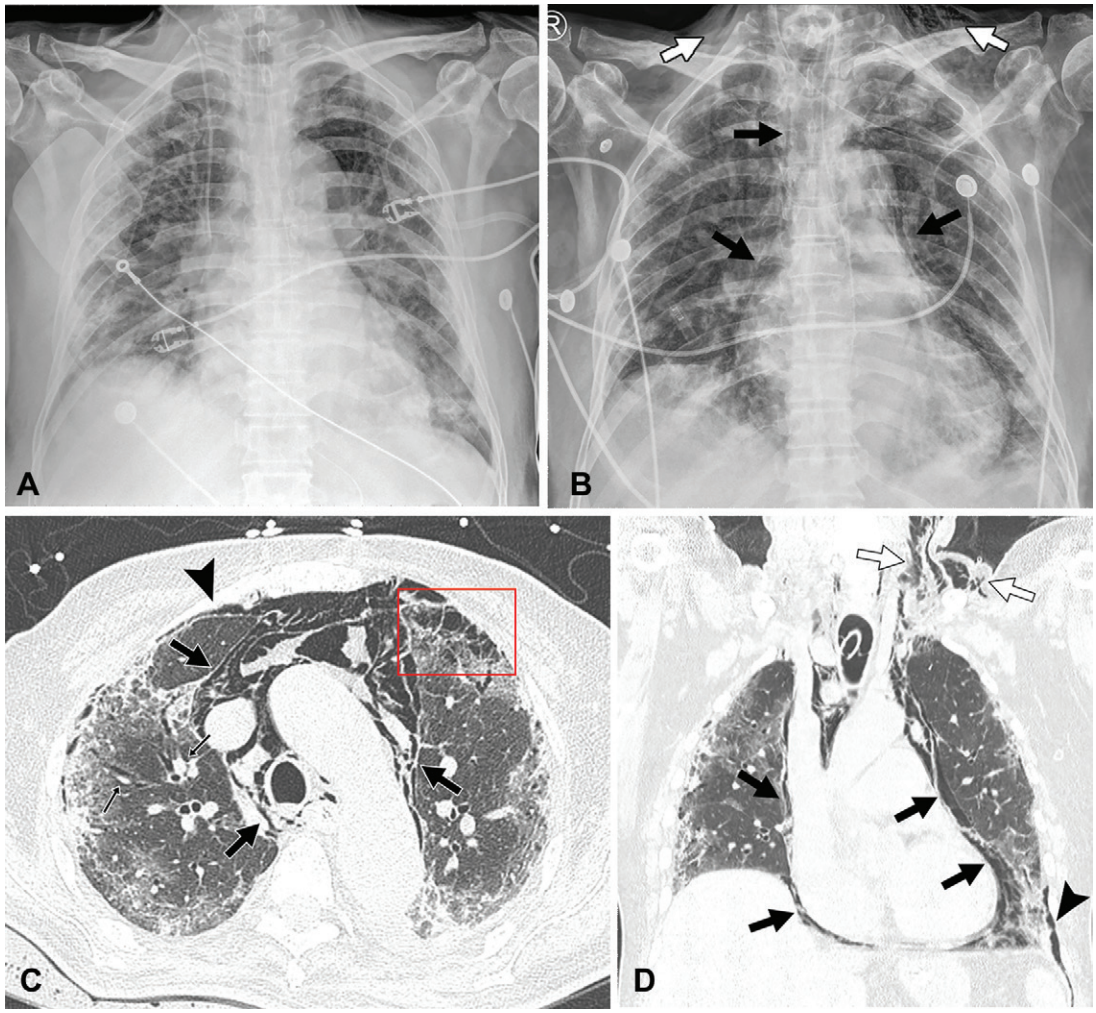

Figure 8: Images of COVID-19 pneumonia with oxygen toxicity and barotrauma at the time of Delta variant–dominant period in a 71-year-old unvaccinated man with diabetes. **(A)** Chest radiograph obtained 10 days after positive nucleic acid amplification test for COVID-19 shows extensive parenchymal opacity involving bilateral lungs. He was transferred to the intensive care unit due to worsening of hypoxemia and was given mechanical ventilation with prolonged oxygen supply. **(B)** Follow-up chest radiograph obtained 25 days after initial diagnosis of COVID-19 demonstrates identifiable pneumomediastinum (black arrows) and subcutaneous emphysema (white arrows) with parenchymal opacities. **(C)** Transverse and **(D)** coronal reformatted images of nonenhanced CT scans depict mixed ground-glass opacity, consolidation, and reticulation in the peripheral areas of both lungs associated with interstitial emphysema (small arrows in **C**) causing Macklin effect, pneumothorax (arrowhead), pneumomediastinum (black arrows) and subcutaneous emphysema (white arrows in **D**). Note air cysts in the anterior left lung (box in **C**). One month after receiving mechanical ventilation with corticosteroid treatment, the patient recovered and was discharged.

tory drugs may lead to pulmonary fungal infections. These include COVID-19–associated pulmonary aspergillosis (CAPA) (88) (Fig 7D, 7E) and COVID-19–associated pulmonary mucormycosis (89). CAPA is defined as invasive pulmonary or tracheobronchial aspergillosis in temporal proximity to a preceding SARS-CoV-2 infection (90). Imaging diagnosis alone is not sufficient to define patients with CAPA because lesions suggestive of CAPA can be hidden or mimicked by lung involvement in patients with severe COVID-19 (Fig 7D, 7E). The most common findings of COVID-19–associated pulmonary mucormycosis are consolidation and cavitation (89). However, these findings are based on a small number of cases or case series. Ongoing or healing pulmonary fungal infections may overlap or obscure CT features of COVID-19 pneumonia.

Pulmonary Thromboembolism

Systemic inflammation, predisposing factors for venous thromboembolism, and endothelial cell damage by SARS-CoV-2 likely predispose to venous and arterial thromboembolism in patients with severe COVID-19. Proinflammatory cytokines such as interleukin 1 and interleukin 6 promote thrombosis by activating platelets and inhibiting fibrinolysis (42). A meta-analysis of 64 503 hospitalized patients with COVID-19 from 102 studies reported that the rate of overall venous thromboembolism and pulmonary thromboembolism was 15% and 8%, respectively (91). The prevalence of venous thromboembolism was significantly higher in patients in the intensive care unit (23% vs 9%). The increase in pulmonary thromboembolism risk was highly dependent on severe COVID-19 (25% vs 15%) in

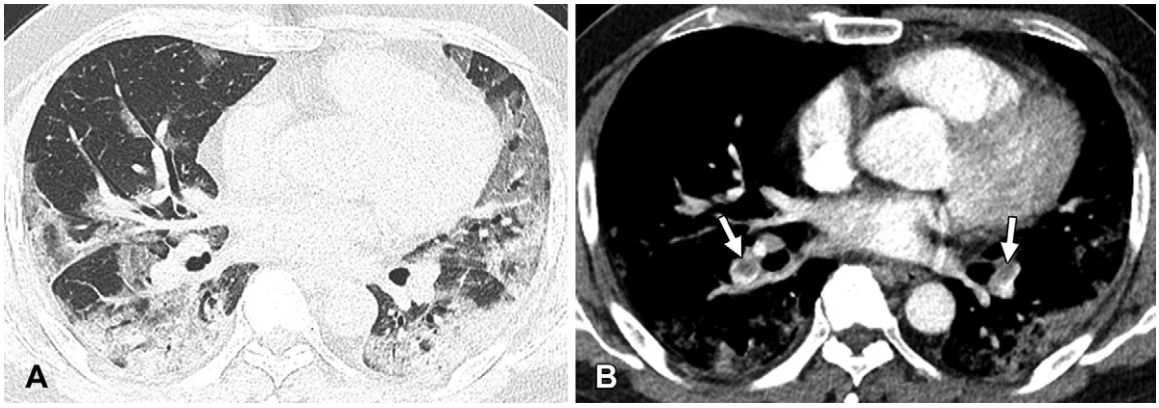

Figure 9: Pulmonary embolisms in a 47-year-old unvaccinated diabetic man with COVID-19 seen at Omicron variant–dominant period. **(A)** Transverse nonenhanced CT scan (lung window) obtained at the level of basal trunks shows bilateral mixed areas of ground-glass opacity and consolidation distributed along bronchovascular bundles or subpleural lungs. **(B)** Contrast-enhanced CT scan (mediastinal window) obtained at a similar level to **A** demonstrates nonocclusive clots in bilateral basal trunk arteries (arrows) along with lung parenchymal lesions.

Table 3: Summary of Current Studies on CT Features in Lung Disease after COVID-19

Study	Patient Cohort	CT Features Up to 3 Months	CT Features at 6 Months	CT Features at 1 Year
Wu et al (101)	83 hospitalized patients with severe COVID-19	Any residual abnormality: 78% (65/83) GGO: 78% (65/83) Reticular lesions: 33% (27/83) Bronchial dilatation: 1% (1/83)	Any residual abnormality: 48% (40/83) GGO: 46% (38/83) Reticular lesions: 16% (13/83) Bronchial dilatation: 1% (1/83)	Any residual abnormality: 24% (20/83) GGO: 23% (19/83) Reticular lesions: 4% (3/83) Bronchial dilatation: 1% (1/83)
Huang et al (98)	1276 hospitalized patients with COVID-19	Not reported	Any residual abnormality: 52% (186/353)	Any residual abnormality: 50% (65/128) of residual abnormality at 6-mo follow-up
Han et al (119)	62 hospitalized patients with severe COVID-19	Not reported	Any residual abnormality: 100% (62/62) GGO: 32% (20/62) Reticular lesions: 58% (36/62) Bronchial dilatation: 44% (27/62)	Any residual abnormality: 73% (45/62) GGO: 11% (7/62) Reticular lesions: 52% (32/62) Bronchial dilatation: 44% (27/62)
Pan et al (102)	209 hospitalized patients with COVID-19	Any residual abnormality: 39% (81/209) GGO: 37% (78/209) Reticular lesions: 15% (31/209) Bronchial dilatation: 12% (25/209)	Any residual abnormality: 26% (56/209) GGO: 25% (53/209) Reticular lesions: 13% (28/209) Bronchial dilatation: 11% (24/209)	Any residual abnormality: 25% (53/209) GGO: 24% (50/209) Reticular lesions: 13% (28/209) Bronchial dilatation: 11% (24/209)
Vijayakumar et al (106)	73 hospitalized patients with COVID-19	Any residual abnormality: 56% (41/73) GGO: 48% (35/73) Reticular lesions: 13% (10/73) Bronchial dilatation: 7% (5/73)	Not reported	Any residual abnormality: 84% (27/32) of residual abnormality at 3-mo follow-up CT
Luger et al (103)	142 hospitalized patients with COVID-19	Any residual abnormality: 63% (54/86) GGO: 58% (50/86) Reticulation: 52% (45/86) Bronchial dilatation: 7% (6/86)	Any residual abnormality: 67% (47/70) GGO: 56% (39/70) Reticular lesions: 56% (39/70) Bronchial dilatation: 9% (6/70)	Any residual abnormality: 54% (49/91) GGO: 44% (40/91) Reticular lesions: 43% (39/91) Bronchial dilatation: 9% (8/91)

Note.—Numbers in parentheses are raw data. GGO = ground-glass opacity.

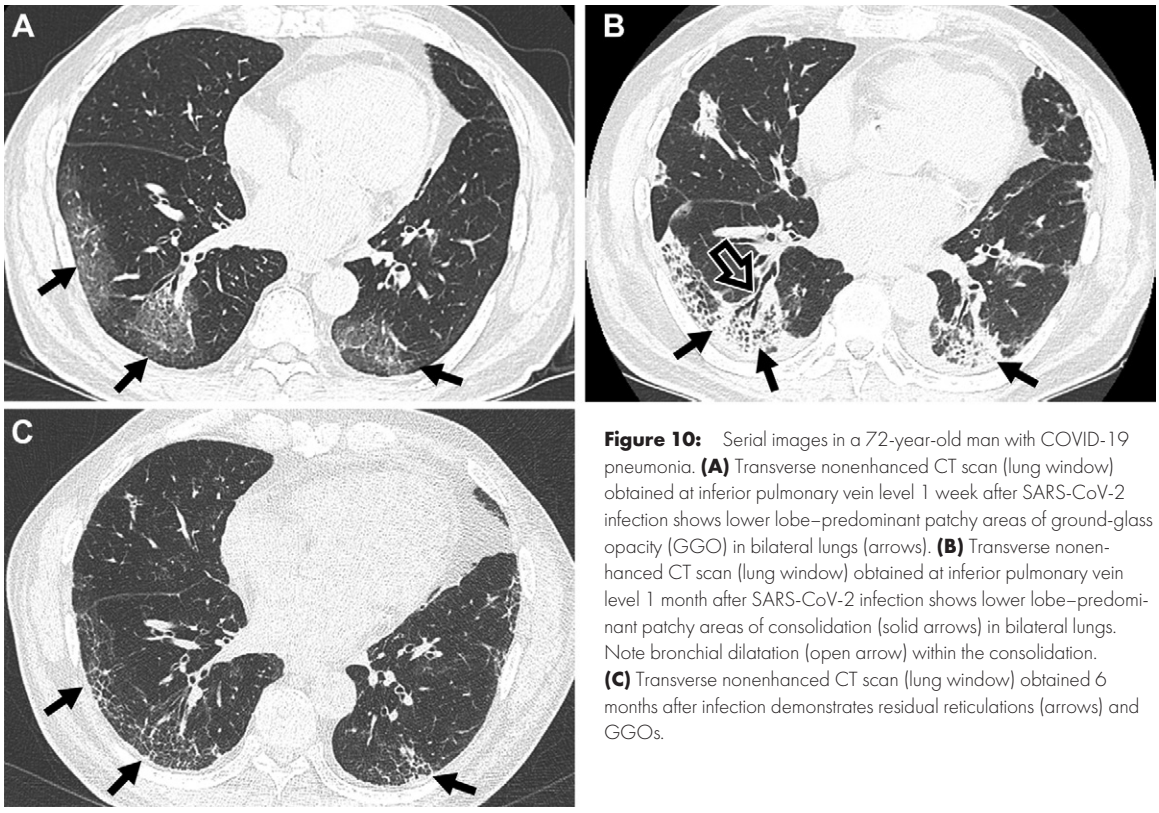

Figure 10: Serial images in a 72-year-old man with COVID-19 pneumonia. **(A)** Transverse nonenhanced CT scan (lung window) obtained at inferior pulmonary vein level 1 week after SARS-CoV-2 infection shows lower lobe–predominant patchy areas of ground-glass opacity (GGO) in bilateral lungs (arrows). **(B)** Transverse nonenhanced CT scan (lung window) obtained at inferior pulmonary vein level 1 month after SARS-CoV-2 infection shows lower lobe–predominant patchy areas of consolidation (solid arrows) in bilateral lungs. Note bronchial dilatation (open arrow) within the consolidation. **(C)** Transverse nonenhanced CT scan (lung window) obtained 6 months after infection demonstrates residual reticulations (arrows) and GGOs.

another meta-analysis (92) (Fig 9). In addition, in an international cohort study of 3358 patients who underwent CT pulmonary angiography, patients with COVID-19 had similar rates of pulmonary thromboembolism compared to patients without COVID-19 (15% in both groups), leading to the recommendation that for patients with COVID-19 and suspected pulmonary thromboembolism, no adjustment to a standard pulmonary thromboembolism diagnostic strategy is required and the same threshold of the D-dimer in the general population could be applied (92–95).

PCC (Long COVID)

Persistent viral infection, delayed resolution of inflammation, and autoimmunity are associated with prolonged symptoms of COVID-19 (96). A report incorporating 10 longitudinal studies found that the proportions of presumed COVID-19 cases ranged from 8% to 17% in patients with suspected or laboratory-confirmed COVID-19 who reported persisting symptoms for more than 12 weeks (97). A cohort study from Wuhan, China, reported that 68% and 49% of survivors of COVID-19 discharged from hospitals reported sequelae symptoms at 6 and 12 months after symptom onset, respectively (98).

In a study comparing the incidence of PCC in patients infected with Omicron and Delta variants (99), 5% and 11% of patients with Omicron and Delta variants infection, respectively, experienced PCC. A lower risk of PCC in the Omicron variant (odds ratio, 0.24–0.50) was consistently observed, regardless of the timing of vaccination (99). Because PCC includes numerous nonrespiratory symptoms, it has been known that only a small portion of patients with PCC have radiologic abnormalities in the chest (100).

Table 3 summarizes the current studies on CT features in lung disease after COVID-19. In a study by Wu and colleagues (101), 48% of patients had residual changes on CT scans at 6 months (Fig 10), 27% at 9 months (Fig 11), and 24% at 12 months (Fig 12). In a study by Huang and colleagues (98), the lung diffusion impairment and radiologic abnormalities persisted for up to 12 months in 36% and 55% of patients, respectively. At 1 year, GGO (76% vs 39%) and interlobular septal thickening (11% vs 0%) were more common in patients who required oxygenation than in those who did not require oxygenation, suggesting that GGO and irregular lines were associated with lung diffusion impairment.

In a study by Pan and colleagues (102), 25% of participants showed abnormal CT findings at 1-year follow-up CT. However, in a study by Luger and colleagues (103), 54% of patients showed CT abnormalities at 1 year after the onset of COVID-19 symptoms, demonstrating extensive GGO, reticulations, bronchial dilation, microcystic changes, or, in 20% of patients, a combination of these (Fig 12). Factors associated with persistent CT abnormalities at 1-year follow-up include older age, male sex, peripheral blood lymphopenia, critical COVID-19 severity, and severe pneumonia and/or ARDS (104).

To summarize the serial follow-up CT studies to date, most residual CT abnormalities are mainly consistent with prior organizing pneumonia and gradually decreased in extent within 3 or 6 months after acute COVID-19 pneumonia, but the residual CT abnormalities showed a tendency of

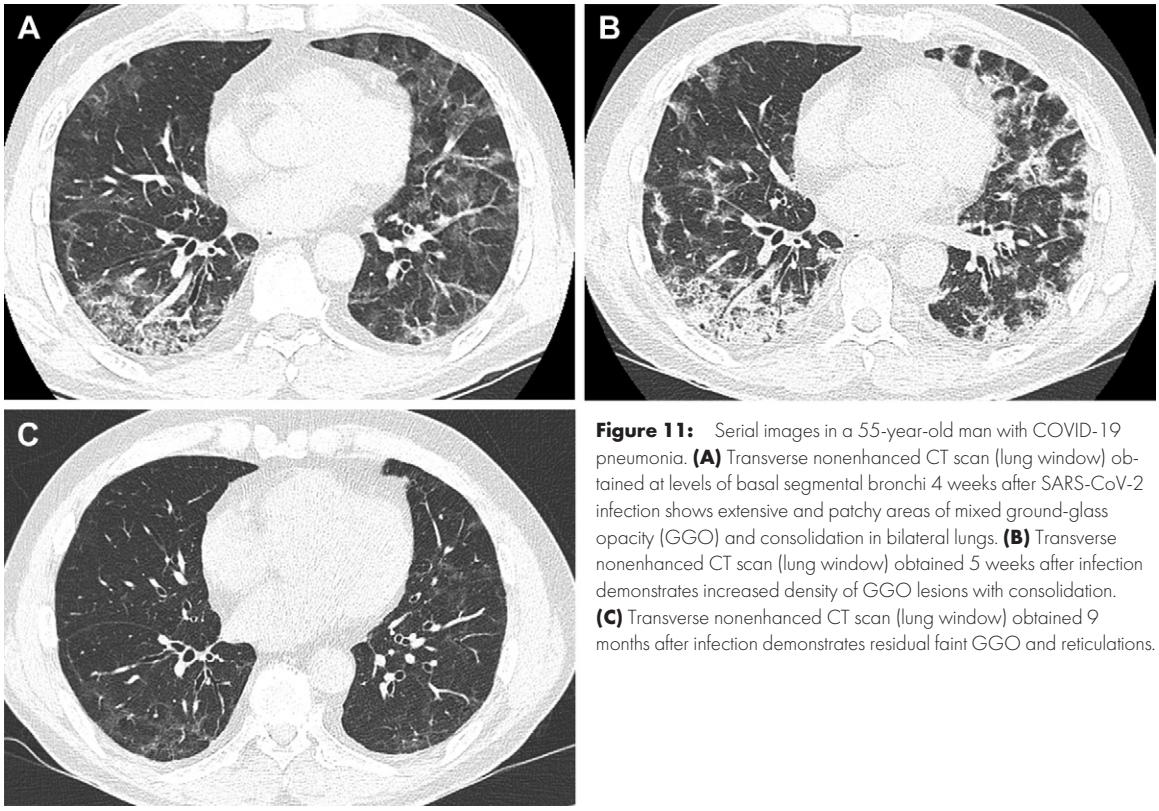

Figure 11: Serial images in a 55-year-old man with COVID-19 pneumonia. **(A)** Transverse nonenhanced CT scan (lung window) obtained at levels of basal segmental bronchi 4 weeks after SARS-CoV-2 infection shows extensive and patchy areas of mixed ground-glass opacity (GGO) and consolidation in bilateral lungs. **(B)** Transverse nonenhanced CT scan (lung window) obtained 5 weeks after infection demonstrates increased density of GGO lesions with consolidation. **(C)** Transverse nonenhanced CT scan (lung window) obtained 9 months after infection demonstrates residual faint GGO and reticulations.

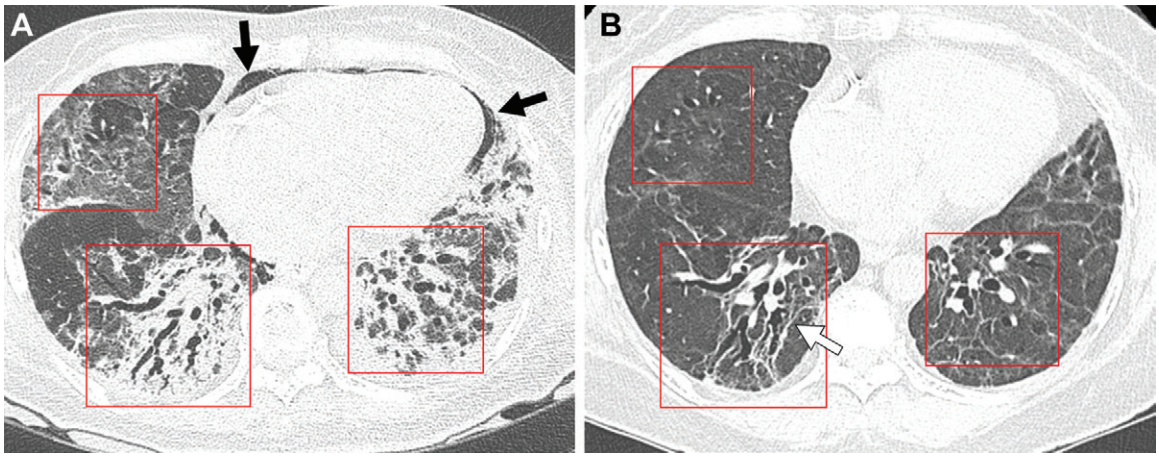

Figure 12: Serial images in a 64-year-old woman with COVID-19 pneumonia. **(A)** Transverse nonenhanced CT scan (lung window) obtained at ventricular level 1 month after SARS-CoV-2 infection shows lower lobe–predominant patchy and wide areas of mixed consolidation and ground-glass opacity (GGO) in bilateral lungs. Note areas of bronchial dilatation (boxes) within parenchymal lesions. Pneumomediastinum (arrows) is also present anteriorly. **(B)** Transverse nonenhanced CT scan (lung window) obtained 12 months after infection demonstrates dilated bronchi (boxes) within remaining GGO lesions. Linear parenchymal bands (arrow) are also noted.

not greatly decreasing after 6 months (98,101–106) (Table 3). Lung abnormality evaluation for at least 6 months might be appropriate to estimate residual lesions of COVID-19 pneumonia, particularly in those having initially severe pneumonia and/or ARDS. At present, because the longest series of follow-up examinations reported does not exceed 12 months, the development of persistent or progressive fibrosis in some individuals cannot yet be excluded (107).

Future Directions

Many deep learning methods have been successfully developed to analyze chest images for various clinical tasks of COVID-19 classification, grading, triage, and survival analysis (Appendix S1) (108–111). In a 2020 study with a data set comprising 4352 chest CT scans (112), the per-scan sensitivity and specificity for detecting COVID-19 were 90% and 96%, respectively (P < .001). These results show that deep learning models can aid

the accurate detection of COVID-19 pneumonia and differentiate the disease from community-acquired pneumonia and other lung conditions. In the earlier course of the epidemic when CT was used for triage of febrile patients, artificial intelligence–aided triage achieved an area under the receiver operating characteristic curve of 0.95, with a sensitivity of 92%, specificity of 85%, positive predictive value of 79%, and negative predictive value of 95%. As for the identification of increases in lesion burden, the artificial intelligence method achieved a sensitivity of 96% and a specificity of 87.5% (113). Lassau and colleagues (114) showed that deep learning analysis provided unique prognostic information for COVID-19 and correlated well with other markers of severity (oxygenation, lactate dehydrogenase level, and C-reactive protein level). Deep learning methods such as artificial intelligence–driven quantification or severity scoring in patients with COVID-19 will be increasingly relevant in COVID-19 management, serving as a noninvasive predictive marker for the clinical course of COVID-19. Artificial intelligence techniques and patient management are described in Appendix S1.

The ongoing COVID-19 pandemic has dramatically changed in the past 3 years as a result of a combination of significant mutations, variable immunity acquired from both infection and vaccination, and improved patient management. Consequently, imaging appearance, severity, and outcomes of COVID-19 pneumonia have changed significantly. Previously described "typical" appearance of COVID-19 pneumonia or COVID-19–associated disease elsewhere in the body may not be relevant in the face of ongoing mutations in SARS-CoV-2 and differences in host immunity. In addition, we are not well aware of the incidence, pathogenesis, or imaging changes over time of PCC and repeat infection. Additional studies of dominant SARS-CoV-2 variants in increasingly vaccinated and previously infected populations of a globally collected clinical and imaging cohort are required, and these could help radiologists contribute to the understanding of interactions between changing viral variants and host immunity (115).

Conclusion

After almost 3 years into the COVID-19 pandemic, we have witnessed the contribution of imaging to this public health crisis. We now have advanced insight into the pathophysiology of COVID-19, vaccines and their usefulness, and imaging features of original, breakthrough, and repeat infections. These insights have led to improved patient management. Much emphasis is given to the continued genetic monitoring of new SARS-CoV-2 variants of concern. Despite advances in knowledge, we encounter patients with PCC who will need long-term follow-up and care. The emerging knowledge of PCC also presents radiology with new motivations and challenges.

Acknowledgments: We are grateful for the transcriptionist Young Joo Moon (Samsung Changwon Hospital, Changwon, South Korea) for her dedicated support of manuscript formatting. We also gratefully acknowledge Miri Jeong, MD, for providing the graphic illustration.

Disclosures of conflicts of interest: Y.J.J. No relevant relationships. **Y.M.W.** No relevant relationships. **H.P.** No relevant relationships. **J.E.L.** No relevant relationships. **S.H.K.** No relevant relationships. **K.S.L.** No relevant relationships.

References

1. WHO Coronavirus disease dashboard. World Health Organization. https://covid19.who.int/. Accessed November 11, 2022.
2. Rubin GD, Ryerson CJ, Haramati LB, et al. The Role of Chest Imaging in Patient Management during the COVID-19 Pandemic: A Multinational Consensus Statement from the Fleischner Society. Radiology 2020;296(1):172–180.
3. Wang W, Xu Y, Gao R, et al. Detection of SARS-CoV-2 in Different Types of Clinical Specimens. JAMA 2020;323(18):1843–1844.
4. Zou L, Ruan F, Huang M, et al. SARS-CoV-2 Viral Load in Upper Respiratory Specimens of Infected Patients. N Engl J Med 2020;382(12):1177–1179.
5. Jeong YJ, Nam BD, Yoo JY, et al. Prognostic Implications of CT Feature Analysis in Patients with COVID-19: a Nationwide Cohort Study. J Korean Med Sci 2021;36(8):e51.
6. Schalekamp S, Bleeker-Rovers CP, Beenen LFM, et al. Chest CT in the Emergency Department for Diagnosis of COVID-19 Pneumonia: Dutch Experience. Radiology 2021;298(2):E98–E106.
7. Revel MP, Parkar AP, Prosch H, et al. COVID-19 patients and the radiology department - advice from the European Society of Radiology (ESR) and the European Society of Thoracic Imaging (ESTI). Eur Radiol 2020;30(9):4903–4909.
8. Dunkle LM, Kotloff KL, Gay CL, et al; 2019nCoV-301 Study Group. Efficacy and Safety of NVX-CoV2373 in Adults in the United States and Mexico. N Engl J Med 2022;386(6):531–543.
9. Dagan N, Barda N, Kepten E, et al. BNT162b2 mRNA Covid-19 Vaccine in a Nationwide Mass Vaccination Setting. N Engl J Med 2021;384(15):1412–1423.
10. Baden LR, El Sahly HM, Essink B, et al; COVE Study Group. Efficacy and Safety of the mRNA-1273 SARS-CoV-2 Vaccine. N Engl J Med 2021;384(5):403–416.
11. CDC COVID-19 Response Team. SARS-CoV-2 B.1.1.529 (Omicron) Variant - United States, December 1-8, 2021. MMWR Morb Mortal Wkly Rep 2021;70(50):1731–1734.
12. Long COVID or Post-COVID Conditions. Centers for Disease Control and Prevention. https://www.cdc.gov/coronavirus/2019-ncov/long-term-effects/index.html. Accessed October 28, 2022.
13. Weiss SR, Leibowitz JL. Coronavirus pathogenesis. Adv Virus Res 2011;81:85–164.
14. Lan J, Ge J, Yu J, et al. Structure of the SARS-CoV-2 spike receptor-binding domain bound to the ACE2 receptor. Nature 2020;581(7807):215–220.
15. Hoffmann M, Kleine-Weber H, Schroeder S, et al. SARS-CoV-2 Cell Entry Depends on ACE2 and TMPRSS2 and Is Blocked by a Clinically Proven Protease Inhibitor. Cell 2020;181(2):271–280.e8.
16. Saheb Sharif-Askari N, Saheb Sharif-Askari F, Alabed M, et al. Airways Expression of SARS-CoV-2 Receptor, ACE2, and TMPRSS2 Is Lower in Children Than Adults and Increases with Smoking and COPD. Mol Ther Methods Clin Dev 2020;18:1–6.
17. Ward IL, Bermingham C, Ayoubkhani D, et al. Risk of covid-19 related deaths for SARS-CoV-2 omicron (B.1.1.529) compared with delta (B.1.617.2): retrospective cohort study. BMJ 2022;378:e070695.
18. Li Q, Guan X, Wu P, et al. Early Transmission Dynamics in Wuhan, China, of Novel Coronavirus-Infected Pneumonia. N Engl J Med 2020;382(13):1199–1207.
19. Shen Y, Li C, Dong H, et al. Community Outbreak Investigation of SARS-CoV-2 Transmission Among Bus Riders in Eastern China. JAMA Intern Med 2020;180(12):1665–1671.
20. Lu J, Gu J, Li K, et al. COVID-19 Outbreak Associated with Air Conditioning in Restaurant, Guangzhou, China, 2020. Emerg Infect Dis 2020;26(7):1628–1631.
21. Hu B, Guo H, Zhou P, Shi ZL. Characteristics of SARS-CoV-2 and COVID-19. Nat Rev Microbiol 2021;19(3):141–154 [Published correction appears in Nat Rev Microbiol 2022;20(5):315.].
22. Siddiqi HK, Mehra MR. COVID-19 illness in native and immunosuppressed states: A clinical-therapeutic staging proposal. J Heart Lung Transplant 2020;39(5):405–407.
23. Li X, Geng M, Peng Y, Meng L, Lu S. Molecular immune pathogenesis and diagnosis of COVID-19. J Pharm Anal 2020;10(2):102–108.
24. Wall EC, Wu M, Harvey R, et al. Neutralising antibody activity against SARS-CoV-2 VOCs B.1.617.2 and B.1.351 by BNT162b2 vaccination. Lancet 2021;397(10292):2331–2333.
25. Zhou D, Dejnirattisai W, Supasa P, et al. Evidence of escape of SARS-CoV-2 variant B.1.351 from natural and vaccine-induced sera. Cell 2021;184(9):2348–2361.e6.

26. Altarawneh HN, Chemaitelly H, Hasan MR, et al. Protection against the Omicron Variant from Previous SARS-CoV-2 Infection. N Engl J Med 2022;386(13):1288–1290.
27. Cao Y, Wang J, Jian F, et al. Omicron escapes the majority of existing SARS-CoV-2 neutralizing antibodies. Nature 2022;602(7898):657–663.
28. Neutralizing antibody levels are highly predictive of immune protection from symptomatic SARS-CoV-2 infection. Nat Med 2021;27(7):1205–1211.
29. Khoury DS, Cromer D, Reynaldi A, et al. Neutralizing antibody levels are highly predictive of immune protection from symptomatic SARS-CoV-2 infection. Nat Med 2021;27(7):1205–1211.
30. Tseng HF, Ackerson BK, Luo Y, et al. Effectiveness of mRNA-1273 against SARS-CoV-2 Omicron and Delta variants. Nat Med 2022;28(5):1063–1071 [Published correction appears in Nat Med 2022;28(5):1095.].
31. Wi YM, Kim SH, Peck KR. An Outbreak of Breakthrough Infections by the SARS-CoV-2 Delta Variant in a Psychiatric Closed Ward. J Korean Med Sci 2022;37(4):e28.
32. Butt AA, Dargham SR, Chemaitelly H, et al. Severity of Illness in Persons Infected With the SARS-CoV-2 Delta Variant vs Beta Variant in Qatar. JAMA Intern Med 2022;182(2):197–205.
33. Karim SSA, Karim QA. Omicron SARS-CoV-2 variant: a new chapter in the COVID-19 pandemic. Lancet 2021;398(10317):2126–2128.
34. Tegally H, Moir M, Everatt J, et al; NGS-SA consortium. Emergence of SARS-CoV-2 Omicron lineages BA.4 and BA.5 in South Africa. Nat Med 2022;28(9):1785–1790.
35. Jørgensen SB, Nygård K, Kacelnik O, Telle K. Secondary Attack Rates for Omicron and Delta Variants of SARS-CoV-2 in Norwegian Households. JAMA 2022;327(16):1610–1611.
36. Tegally H, Moir M, Everatt J, et al. Continued Emergence and Evolution of Omicron in South Africa: New BA.4 and BA.5 lineages. Preprint medRxiv. Posted May 2, 2022. Accessed November 20, 2022.
37. Khan K, Karim F, Ganga Y, et al. Omicron sub-lineages BA.4/BA.5 escape BA.1 infection elicited neutralizing immunity. Preprint at medRxiv. Posted May 1, 2022. Accessed November 20, 2022.
38. Muhsen K, Maimon N, Mizrahi AY, et al. Association of Receipt of the Fourth BNT162b2 Dose With Omicron Infection and COVID-19 Hospitalizations Among Residents of Long-term Care Facilities. JAMA Intern Med 2022;182(8):859–867.
39. WHO COVID-19 Case definition. World Health Organization. https://www.who.int/publications/i/item/WHO-2019-nCoV-Surveillance_Case_Definition-2022.1. Published July 22, 2022. Accessed September 18, 2022.
40. Use of chest imaging in COVID-19: a rapid advice guide, 11 June 2020. World Health Organization. https://www.who.int/publications/i/item/use-of-chest-imaging-in-covid-19. Published June 11, 2020. Accessed September 7, 2022.
41. McMillan P, Dexhiemer T, Neubig RR, Uhal BD. COVID-19-A Theory of Autoimmunity Against ACE-2 Explained. Front Immunol 2021;12:582166.
42. Gupta A, Madhavan MV, Sehgal K, et al. Extrapulmonary manifestations of COVID-19. Nat Med 2020;26(7):1017–1032.
43. Lee JE, Hwang M, Kim YH, et al. Imaging and Clinical Features of COVID-19 Breakthrough Infections: A Multicenter Study. Radiology 2022;303(3):682–692.
44. Sadiq Z, Rana S, Mahfoud Z, Raoof A. Systematic review and meta-analysis of chest radiograph (CXR) findings in COVID-19. Clin Imaging 2021;80:229–238.
45. Petrilli CM, Jones SA, Yang J, et al. Factors associated with hospital admission and critical illness among 5279 people with coronavirus disease 2019 in New York City: prospective cohort study. BMJ 2020;369:m1966.
46. Au-Yong I, Higashi Y, Giannotti E, et al. Chest Radiograph Scoring Alone or Combined with Other Risk Scores for Predicting Outcomes in COVID-19. Radiology 2022;302(2):460–469.
47. WHO Rapid Evidence Appraisal for COVID-19 Therapies Working Group; Sterne JAC, Murthy S, et al. Association Between Administration of Systemic Corticosteroids and Mortality Among Critically Ill Patients With COVID-19: A Meta-analysis. JAMA 2020;324(13):1330–1341.
48. RECOVERY Collaborative Group; Horby P, Lim WS, et al. Dexamethasone in Hospitalized Patients with Covid-19. N Engl J Med 2021;384(8):693–704.
49. Ai T, Yang Z, Hou H, et al. Correlation of Chest CT and RT-PCR Testing for Coronavirus Disease 2019 (COVID-19) in China: A Report of 1014 Cases. Radiology 2020;296(2):E32–E40.
50. Fang Y, Zhang H, Xie J, et al. Sensitivity of Chest CT for COVID-19: Comparison to RT-PCR. Radiology 2020;296(2):E115–E117.
51. Revel MP, Boussouar S, de Margerie-Mellon C, et al. Study of Thoracic CT in COVID-19: The STOIC Project. Radiology 2021;301(1):E361–E370.
52. Kwee TC, Kwee RM. Chest CT in COVID-19: What the Radiologist Needs to Know. RadioGraphics 2020;40(7):1848–1865.
53. Yoon SH, Lee KH, Kim JY, et al. Chest Radiographic and CT Findings of the 2019 Novel Coronavirus Disease (COVID-19): Analysis of Nine Patients Treated in Korea. Korean J Radiol 2020;21(4):494–500.
54. Salehi S, Abedi A, Balakrishnan S, Gholamrezanezhad A. Coronavirus disease 2019 (COVID-19) imaging reporting and data system (COVID-RADS) and common lexicon: a proposal based on the imaging data of 37 studies. Eur Radiol 2020;30(9):4930–4942.
55. Prokop M, van Everdingen W, van Rees Vellinga T, et al. CO-RADS: A Categorical CT Assessment Scheme for Patients Suspected of Having COVID-19-Definition and Evaluation. Radiology 2020;296(2):E97–E104.
56. Simpson S, Kay FU, Abbara S, et al. Radiological Society of North America Expert Consensus Document on Reporting Chest CT Findings Related to COVID-19: Endorsed by the Society of Thoracic Radiology, the American College of Radiology, and RSNA. Radiol Cardiothorac Imaging 2020;2(2):e200152.
57. Rodrigues JCL, Hare SS, Edey A, et al. An update on COVID-19 for the radiologist - A British society of Thoracic Imaging statement. Clin Radiol 2020;75(5):323–325.
58. Lieveld AWE, Azijli K, Teunissen BP, et al. Chest CT in COVID-19 at the ED: Validation of the COVID-19 Reporting and Data System (CO-RADS) and CT Severity Score: A Prospective, Multicenter, Observational Study. Chest 2021;159(3):1126–1135.
59. Abdel-Tawab M, Basha MAA, Mohamed IAI, et al. Comparison of the CO-RADS and the RSNA chest CT classification system concerning sensitivity and reliability for the diagnosis of COVID-19 pneumonia. Insights Imaging 2021;12(1):55.
60. Bergwerk M, Gonen T, Lustig Y, et al. Covid-19 Breakthrough Infections in Vaccinated Health Care Workers. N Engl J Med 2021;385(16):1474–1484.
61. Butt AA, Khan T, Yan P, Shaikh OS, Omer SB, Mayr F. Rate and risk factors for breakthrough SARS-CoV-2 infection after vaccination. J Infect 2021;83(2):237–279.
62. Hacisuleyman E, Hale C, Saito Y, et al. Vaccine Breakthrough Infections with SARS-CoV-2 Variants. N Engl J Med 2021;384(23):2212–2218.
63. Nixon DF, Ndhlovu LC. Vaccine Breakthrough Infections with SARS-CoV-2 Variants. N Engl J Med 2021;385(2):e7.
64. Menni C, Valdes AM, Polidori L, et al. Symptom prevalence, duration, and risk of hospital admission in individuals infected with SARS-CoV-2 during periods of omicron and delta variant dominance: a prospective observational study from the ZOE COVID Study. Lancet 2022;399(10335):1618–1624.
65. Akkız H. The Biological Functions and Clinical Significance of SARS-CoV-2 Variants of Corcern. Front Med (Lausanne) 2022;9:849217.
66. Nyberg T, Ferguson NM, Nash SG, et al. Comparative analysis of the risks of hospitalisation and death associated with SARS-CoV-2 omicron (B.1.1.529) and delta (B.1.617.2) variants in England: a cohort study. Lancet 2022;399(10332):1303–1312.
67. Lee JE, Hwang M, Kim YH, et al. SARS-CoV-2 Variants Infection in Relationship to Imaging-based Pneumonia and Clinical Outcomes. Radiology 2022. 10.1148/radiol.221795. Published online September 27, 2022.
68. Yoon SH, Lee JH, Kim BN. Chest CT Findings in Hospitalized Patients with SARS-CoV-2: Delta versus Omicron Variants. Radiology 2022. 10.1148/radiol.220676. Published online June 28, 2022.
69. Lawandi A, Warner S, Sun J, et al. Suspected Severe Acute Respiratory Syndrome Coronavirus 2 (SARS-COV-2) Reinfections: Incidence, Predictors, and Healthcare Use Among Patients at 238 US Healthcare Facilities, 1 June 2020 to 28 February 2021. Clin Infect Dis 2022;74(8):1489–1492.
70. Jang EJ, Choe YJ, Yun GW, et al. Reinfection with SARS-CoV-2 in general population, South Korea; nationwide retrospective cohort study. J Med Virol 2022;94(11):5589–5592.
71. Slezak J, Bruxvoort K, Fischer H, Broder B, Ackerson B, Tartof S. Rate and severity of suspected SARS-Cov-2 reinfection in a cohort of PCR-positive COVID-19 patients. Clin Microbiol Infect 2021;27(12):1860.e7–1860.e10.
72. Cavanaugh AM, Spicer KB, Thoroughman D, Glick C, Winter K. Reduced Risk of Reinfection with SARS-CoV-2 After COVID-19 Vaccination - Kentucky, May-June 2021. MMWR Morb Mortal Wkly Rep 2021;70(32):1081–1083.
73. Malato J, Ribeiro RM, Leite PP, et al. Risk of BA.5 Infection among Persons Exposed to Previous SARS-CoV-2 Variants. N Engl J Med 2022;387(10):953–954.
74. Shastri J, Parikh S, Aggarwal V, et al. Severe SARS-CoV-2 Breakthrough Reinfection With Delta Variant After Recovery From Breakthrough Infection by Alpha Variant in a Fully Vaccinated Health Worker. Front Med (Lausanne) 2021;8:737007.
75. Katal S, Myers L, Gholamrezanezhad A. SARS-CoV-2 reinfection: "New baseline" imaging concept in the era of COVID-19. Clin Imaging 2021;78:142–145.

76. Langerbeins P, Hallek M. COVID-19 in patients with hematologic malignancy. Blood 2022;140(3):236–252.
77. Bhaskaran K, Rentsch CT, MacKenna B, et al. HIV infection and COVID-19 death: a population-based cohort analysis of UK primary care data and linked national death registrations within the OpenSAFELY platform. Lancet HIV 2021;8(1):e24–e32.
78. Hadi YB, Naqvi SFZ, Kupec JT, Sofka S, Sarwari A. Outcomes of COVID-19 in Solid Organ Transplant Recipients: A Propensity-matched Analysis of a Large Research Network. Transplantation 2021;105(6):1365–1371.
79. Grainger R, Kim AHJ, Conway R, Yazdany J, Robinson PC. COVID-19 in people with rheumatic diseases: risks, outcomes, treatment considerations. Nat Rev Rheumatol 2022;18(4):191–204.
80. Hochhegger B, Pelaez A, Machuca T, et al. CT imaging findings in lung transplant recipients with COVID-19. Eur Radiol 2022. 10.1007/s00330-022-09148-w. Published online September 24, 2022.
81. Huang QS, Wood T, Jelley L, et al. Impact of the COVID-19 nonpharmaceutical interventions on influenza and other respiratory viral infections in New Zealand. Nat Commun 2021;12(1):1001.
82. Australian Government Department of Health. Australian influenca surveillance report. https://www.health.gov.au/sites/default/files/documents/2022/10/aisr-fortnightly-report-no-7-20-june-to-3-july-2022.pdf. Accessed October 28, 2022.
83. Yin Z, Kang Z, Yang D, Ding S, Luo H, Xiao E. A Comparison of Clinical and Chest CT Findings in Patients With Influenza A (H1N1) Virus Infection and Coronavirus Disease (COVID-19). AJR Am J Roentgenol 2020;215(5):1065–1071.
84. Zompatori M, Ciccarese F, Fasano L. Overview of current lung imaging in acute respiratory distress syndrome. Eur Respir Rev 2014;23(134):519–530.
85. Lemmers DHL, Abu Hilal M, Bnà C, et al. Pneumomediastinum and subcutaneous emphysema in COVID-19: barotrauma or lung frailty? ERJ Open Res 2020;6(4):00385–2020.
86. Palumbo D, Campochiaro C, Belletti A, et al; COVID-BioB Study Group. Pneumothorax/pneumomediastinum in non-intubated COVID-19 patients: Differences between first and second Italian pandemic wave. Eur J Intern Med 2021;88:144–146.
87. Paternoster G, Belmonte G, Scarano E, et al; COVID-Macklin Study Group. Macklin effect on baseline chest CT scan accurately predicts barotrauma in COVID-19 patients. Respir Med 2022;197:106853.
88. Dewi IM, Janssen NA, Rosati D, et al. Invasive pulmonary aspergillosis associated with viral pneumonitis. Curr Opin Microbiol 2021;62:21–27.
89. Garg M, Prabhakar N, Muthu V, et al. CT Findings of COVID-19-associated Pulmonary Mucormycosis: A Case Series and Literature Review. Radiology 2022;302(1):214–217.
90. Koehler P, Bassetti M, Chakrabarti A, et al; Infectious Disease Canada. Defining and managing COVID-19-associated pulmonary aspergillosis: the 2020 ECMM/ISHAM consensus criteria for research and clinical guidance. Lancet Infect Dis 2021;21(6):e149–e162.
91. Tan BK, Mainbourg S, Friggeri A, et al. Arterial and venous thromboembolism in COVID-19: a study-level meta-analysis. Thorax 2021;76(10):970–979.
92. Suh YJ, Hong H, Ohana M, et al. Pulmonary Embolism and Deep Vein Thrombosis in COVID-19: A Systematic Review and Meta-Analysis. Radiology 2021;298(2):E70–E80.
93. Freund Y, Drogrey M, Miró Ò, et al; IMPROVING EMERGENCY CARE FHU Collaborators. Association Between Pulmonary Embolism and COVID-19 in Emergency Department Patients Undergoing Computed Tomography Pulmonary Angiogram: The PEPCOV International Retrospective Study. Acad Emerg Med 2020;27(9):811–820.
94. Freund Y, Cohen-Aubart F, Bloom B. Acute Pulmonary Embolism: A Review. JAMA 2022;328(13):1336–1345.
95. Revel MP, Beeker N, Porcher R, et al; AP-HP /Universities/Inserm COVID-19 research collaboration, AP-HP Covid CDR Initiative. What level of D-dimers can safely exclude pulmonary embolism in COVID-19 patients presenting to the emergency department? Eur Radiol 2022;32(4):2704–2712.
96. Mehandru S, Merad M. Pathological sequelae of long-haul COVID. Nat Immunol 2022;23(2):194–202.
97. Thompson EJ, Williams DM, Walker AJ, et al; OpenSAFELY Collaborative. Long COVID burden and risk factors in 10 UK longitudinal studies and electronic health records. Nat Commun 2022;13(1):3528.
98. Huang L, Yao Q, Gu X, et al. 1-year outcomes in hospital survivors with COVID-19: a longitudinal cohort study. Lancet 2021;398(10302):747–758 [Published correction appears in Lancet 2022;399(10337):1778.].
99. Antonelli M, Pujol JC, Spector TD, Ourselin S, Steves CJ. Risk of long COVID associated with delta versus omicron variants of SARS-CoV-2. Lancet 2022;399(10343):2263–2264.
100. Myall KJ, Mukherjee B, Castanheira AM, et al. Persistent Post-COVID-19 Interstitial Lung Disease. An Observational Study of Corticosteroid Treatment. Ann Am Thorac Soc 2021;18(5):799–806.
101. Wu X, Liu X, Zhou Y, et al. 3-month, 6-month, 9-month, and 12-month respiratory outcomes in patients following COVID-19-related hospitalisation: a prospective study. Lancet Respir Med 2021;9(7):747–754.
102. Pan F, Yang L, Liang B, et al. Chest CT Patterns from Diagnosis to 1 Year of Follow-up in Patients with COVID-19. Radiology 2022;302(3):709–719.
103. Luger AK, Sonnweber T, Gruber L, et al. Chest CT of Lung Injury 1 Year after COVID-19 Pneumonia: The CovILD Study. Radiology 2022;304(2):462–470.
104. Lee KS, Wi YM. Residual Lung Lesions at 1-year CT after COVID-19. Radiology 2022;302(3):720–721.
105. Drake TM, Docherty AB, Harrison EM, et al; ISARIC4C Investigators. Outcome of Hospitalization for COVID-19 in Patients with Interstitial Lung Disease. An International Multicenter Study. Am J Respir Crit Care Med 2020;202(12):1656–1665.
106. Vijayakumar B, Tonkin J, Devaraj A, et al. CT Lung Abnormalities after COVID-19 at 3 Months and 1 Year after Hospital Discharge. Radiology 2022;303(2):444–454.
107. Martini K, Larici AR, Revel MP, et al; European Society of Thoracic Imaging (ESTI), the European Society of Radiology (ESR). COVID-19 pneumonia imaging follow-up: when and how? A proposition from ESTI and ESR. Eur Radiol 2022;32(4):2639–2649.
108. Wang H, Wang L, Lee EH, et al. Decoding COVID-19 pneumonia: comparison of deep learning and radiomics CT image signatures. Eur J Nucl Med Mol Imaging 2021;48(5):1478–1486 [Published correction appears in Eur J Nucl Med Mol Imaging 2021;48(5):1697.].
109. Kwon YJF, Toussie D, Finkelstein M, et al. Combining Initial Radiographs and Clinical Variables Improves Deep Learning Prognostication in Patients with COVID-19 from the Emergency Department. Radiol Artif Intell 2020;3(2):e200098.
110. Li MD, Arun NT, Gidwani M, et al. Automated Assessment and Tracking of COVID-19 Pulmonary Disease Severity on Chest Radiographs using Convolutional Siamese Neural Networks. Radiol Artif Intell 2020;2(4):e200079.
111. Chassagnon G, Vakalopoulou M, Battistella E, et al. AI-driven quantification, staging and outcome prediction of COVID-19 pneumonia. Med Image Anal 2021;67:101860.
112. Li L, Qin L, Xu Z, et al. Using Artificial Intelligence to Detect COVID-19 and Community-acquired Pneumonia Based on Pulmonary CT: Evaluation of the Diagnostic Accuracy. Radiology 2020;296(2):E65–E71.
113. Wang M, Xia C, Huang L, et al. Deep learning-based triage and analysis of lesion burden for COVID-19: a retrospective study with external validation. Lancet Digit Health 2020;2(10):e506–e515.
114. Lassau N, Ammari S, Chouzenoux E, et al. Integrating deep learning CT-scan model, biological and clinical variables to predict severity of COVID-19 patients. Nat Commun 2021;12(1):634.
115. Little BP. Variants and Vaccination in COVID-19: New Complexities and Challenges for Radiology Research and Practice. Radiology 2022. 10.1148/radiol.222478. Published online October 18, 2022.
116. Liu L, Iketani S, Guo Y, et al. Striking antibody evasion manifested by the Omicron variant of SARS-CoV-2. Nature 2022;602(7898):676–681.
117. Tsakok MT, Watson RA, Saujani SJ, et al. Chest CT and Hospital Outcomes in Patients with Omicron Compared with Delta Variant SARS-CoV-2 Infection. Radiology 2022. 10.1148/radiol.220533. Published online June 21, 2022.
118. Penha D, Pinto EG, Matos F, et al. CO-RADS: Coronavirus Classification Review. J Clin Imaging Sci 2021;11:9.
119. Han X, Fan Y, Alwalid O, et al. Fibrotic Interstitial Lung Abnormalities at 1-year Follow-up CT after Severe COVID-19. Radiology 2021;301(3):E438–E440.